The Arabidopsis Class III Peroxidase AtPRX71 Negatively Regulates Growth under Physiological Conditions and in Response to Cell Wall Damage[1][OPEN]

Sara Raggi, Alberto Ferrarini, Massimo Delledonne, Christophe Dunand, Philippe Ranocha, Giulia De Lorenzo, Felice Cervone, and Simone Ferrari*

Institute Pasteur-Fondazione Cenci Bolognetti and Dipartimento di Biologia e Biotecnologie "Charles Darwin," Sapienza Università di Roma, 00185 Rome, Italy (S.R., G.D.L., F.C., S.F.); Dipartimento di Biotecnologie, Università degli Studi di Verona, 37134 Verona, Italy (A.F., M.D.); Université de Toulouse, Université Paul Sabatier, Unité Mixte de Recherche 5546, Laboratoire de Recherche en Sciences Végétales, F–31326 Castanet-Tolosan, France (C.D., P.R.); and Centre National de la Recherche Scientifique, Unité Mixte de Recherche 5546, F–31326 Castanet-Tolosan, France (C.D., P.R.)

ORCID IDs: 0000-0002-8452-3380 (A.F.); 0000-0002-7100-4581 (M.D.); 0000-0003-1637-4042 (C.D.); 0000-0002-1707-5418 (G.D.L.); 0000-0001-8141-5352 (F.C.); 0000-0002-1389-2090 (S.F.).

The structure of the cell wall has a major impact on plant growth and development, and alteration of cell wall structural components is often detrimental to biomass production. However, the molecular mechanisms responsible for these negative effects are largely unknown. Arabidopsis (*Arabidopsis thaliana*) plants with altered pectin composition because of either the expression of the *Aspergillus niger* polygalacturonase II (AnPGII; *35S:AnPGII* plants) or a mutation in the *QUASIMODO2* (*QUA2*) gene that encodes a putative pectin methyltransferase (*qua2-1* plants), display severe growth defects. Here, we show that expression of Arabidopsis *PEROXIDASE71* (*AtPRX71*), encoding a class III peroxidase, strongly increases in *35S:AnPGII* and *qua2-1* plants as well as in response to treatments with the cellulose synthase inhibitor isoxaben, which also impairs cell wall integrity. Analysis of *atprx71* loss-of-function mutants and plants overexpressing *AtPRX71* indicates that this gene negatively influences Arabidopsis growth at different stages of development, likely limiting cell expansion. The *atprx71-1* mutation partially suppresses the dwarf phenotype of *qua2-1*, suggesting that *AtPRX71* contributes to the growth defects observed in plants undergoing cell wall damage. Furthermore, *AtPRX71* seems to promote the production of reactive oxygen species in *qua2-1* plants as well as plants treated with isoxaben. We propose that AtPRX71 contributes to strengthen cell walls, therefore restricting cell expansion, during normal growth and in response to cell wall damage.

The cell wall is a complex, multifunctional and dynamic structure that provides mechanical support to plant cells, and it is involved in cell adhesion, defense against pathogens, regulation of metabolic functions, and cell-to-cell communication (Keegstra, 2010). Cell walls are usually composed of polysaccharides (cellulose, hemicelluloses, and pectins), phenolic compounds (e.g. ferulic acid and lignin), and proteins (Carpita and McCann, 2000). In the apoplast, cellulose microfibrils are associated to hemicelluloses, such as xyloglucans (XGs), producing a network embedded in a matrix of pectins. The latter are mainly composed of linear chains of homogalacturonan (HG) and branched chains of rhamnogalacturonans. Pectins are abundant in the middle lamella, where they ensure cell adhesion, as well as in primary and, to a lesser degree, secondary walls (Willats et al., 2001). HG is synthesized in a highly esterified form in the Golgi apparatus (Zhang and Staehelin, 1992) and then secreted in the apoplast, where pectin methylesterases remove part of the methyl groups (Pelloux et al., 2007). Free carboxylic groups allow the formation of so-called egg box structures, in which adjacent HG chains are linked by calcium-mediated ionic bridges, making the pectin matrix more rigid (Micheli, 2001). Pectins can also form other types of interactions, such as covalent cross links with other cell wall polysaccharides, phenolic compounds, and proteins (Caffall and Mohnen, 2009; Tan et al., 2013).

The wall structure influences both the extent and the direction of cell expansion (Mirabet et al., 2011). Growth takes place perpendicularly to the direction of

[1] This work was supported by the Fondazione Cariverona Completamento e attività del Centro di Genomica Funzionale Vegetale (to A.F. and M.D.), the Université Paul Sabatier Toulouse 3 (to C.D.), the Centre National de la Recherche Scientifique (to P.R.), the Ministero delle Politiche Agricole, Alimentari e Forestali Grant BIOMASSVAL (to F.C.), and the Institute Pasteur-Fondazione Cenci Bolognetti (to F.C.).

* Address correspondence to simone.ferrari@uniroma1.it.

The author responsible for distribution of materials integral to the findings presented in this article in accordance with the policy described in the Instructions for Authors (www.plantphysiol.org) is: Simone Ferrari (simone.ferrari@uniroma1.it).

S.R., M.D., C.D., G.D.L., and F.C. designed the research; S.R., A.F., P.R., and S.F. performed the experiments; S.R., A.F., C.D., and P.R. analyzed the data; S.R., C.D., and S.F. wrote the article with comments from all of the authors.

[OPEN] Articles can be viewed without a subscription.

www.plantphysiol.org/cgi/doi/10.1104/pp.15.01464

cellulose microfibrils, which are deposited along the perpendicular axis of the cell, providing resistance to turgor pressure and extensibility along the longitudinal axis (Crowell et al., 2010). Two major classes of proteins have been proposed to promote cell wall expansion: XG endotransglycosylases, which cleave XG chains and link together the newly generated reduced end to a new XG chain (Fry et al., 1992), and expansins, which promote primary cell walls relaxation by disrupting cellulose-hemicellulose noncovalent links (Cosgrove, 2000). During expansion, the cell wall is relaxed, whereas turgor forces induce its deformation; subsequently, expansin inhibition and formation of cross links between structural proteins (such as extensins), polysaccharides, and/or monolignols cause wall stiffening and, consequently, slow down expansion (Wolf et al., 2009).

Regulation of apoplastic levels of reactive oxygen species (ROS) is important to determine cell expansion rate and organ size (Gapper and Dolan, 2006). ROS production in the cell wall is controlled, both under physiological conditions and in response to environmental stimuli, by several classes of enzymes, most prominently plasma membrane NADPH oxidases (Torres and Dangl, 2005) and class III peroxidases (CIII Prxs; Bolwell et al., 1999; Cosio and Dunand, 2009). NADPH oxidases, commonly known as respiratory burst oxidase homologs (Rbohs), are transmembrane proteins that oxidize cytoplasmic NADPH, translocate electrons across the plasma membrane, and generate superoxide radicals in the cell wall (Torres et al., 2002; Torres and Dangl, 2005). Superoxide radicals are then rapidly converted into hydrogen peroxide (H_2O_2) either spontaneously or in a reaction catalyzed by superoxide dismutases (Bolwell et al., 1999).

CIII Prxs are heme-containing enzymes secreted in the extracellular space or the vacuole, where they perform two different enzymatic cycles, namely the peroxidative and hydroxylic cycles (Welinder et al., 2002; Passardi et al., 2004). During the peroxidative cycle, the enzyme uses H_2O_2 as an oxidant in a two-step reaction to convert different substrates, including cell wall phenolic compounds and structural proteins, into free radicals that can subsequently combine together to form covalent linkages. This activity contributes to cell wall stiffening and therefore limits growth. CIII Prxs can also cause cell wall loosening through the hydroxylic cycle, in which H_2O_2 and O_2^- are used in a Fenton-type reaction to generate hydroxyl radicals, including $^{\bullet}OH$, that lead to nonenzymatic cleavage of polysaccharides (Chen and Schopfer, 1999; Dunand et al., 2003; Passardi et al., 2005). CIII Prxs can, therefore, play opposite roles in cell expansion, being able to cause both wall stiffening and loosening, depending on the growth conditions. CIII Prxs can also generate O_2^-, which is then dismutated into H_2O_2, through the oxidation of NAD(P)H. These enzymes can both positively and negatively modulate apoplastic ROS levels (Passardi et al., 2004).

The enzymatic characteristics of CIII Prxs allow them to participate in a wide range of physiological processes, including seed germination, plant growth, and elongation and defense against pathogens, as well as the catabolism of several extracellular molecules, including auxins (Hiraga et al., 2001). CIII Prxs are also involved in lignification through the H_2O_2-dependent generation of monolignol phenoxy radicals that spontaneously form lignin polymers (Marjamaa et al., 2009). Lignin monomers can also cross link cell wall polysaccharides, including pectins, through ferulate bridges or diferulate bonds formed by CIII Prxs in the presence of H_2O_2 (Iiyama et al., 1994). Notably, in some plant species, CIII Prxs-mediated cross links between ferulic acid and pectins arrest cell expansion (Iiyama et al., 1994). Lastly, CIII Prxs can cross link Tyr and Lys residues of extensins, contributing to the formation of a dense network within the cell wall (Schnabelrauch et al., 1996).

CIII Prxs likely appeared when plants colonized land and subsequently underwent a high rate of gene duplication, with the consequent increase of functional specialization (Passardi et al., 2005). For instance, the Arabidopsis (*Arabidopsis thaliana*) genome encodes 73 putative CIII Prxs, with various spatiotemporal expression profiles, suggesting that different isoforms play specific roles in growth, development, and adaptation to the environment (Tognolli et al., 2002; Welinder et al., 2002). In this article, we show that the Arabidopsis CIII Prx gene *AtPRX71*, which is strongly expressed upon loss of cell wall integrity (CWI), negatively affects growth and cell size and positively regulates ROS levels. In addition, when *AtPRX71* is lacking, both ROS accumulation and growth defects caused by cell wall alterations are significantly reduced. We propose that accumulation of ROS-generating CIII Prxs is a mechanism to cope with loss of CWI both during normal development and in response to stress, leading to wall stiffening and therefore limiting cell expansion and growth.

RESULTS

Levels of *AtPRX71* Transcripts Are Higher in Plants with Altered Cell Walls

We have previously shown that tobacco (*Nicotiana tabacum*) and Arabidopsis plants expressing an attenuated version of the *Aspergillus niger* polygalacturonase II (AnPGII; *35S*:*AnPGII* plants) have a reduced content of deesterified HG and a significant reduction of growth that correlates with the levels of expression of the transgene (Capodicasa et al., 2004). Furthermore, *35S*:*AnPGII* plants show constitutive activation of defense responses and accumulation of high levels of ROS in their tissues (Ferrari et al., 2008). To obtain insights into the mechanisms underlying the growth defect of *35S*:*AnPGII* plants, whole-genome transcript analysis of rosette leaves of two independent transgenic lines, *35S*:*AnPGII* 57 and 26, that show high levels of expression of the transgene (Lionetti et al., 2010) was performed using custom Arabidopsis 28K microarrays (GenBank Gene Expression Omnibus [GEO] Platform ID no. GPL15543). Differentially expressed transcripts were identified using a false discovery rate (FDR) < 0.05 and a module of logged fold change (FC) on base 2 ($|\log_2 FC| \geq 1$ (GEO accession no. GSE66980). With this filtering criteria, the

transcript levels of 16 genes increased, and those of 4 genes decreased in a statistically significant way in rosette leaves of both transgenic lines compared with the wild type (Table I). Gene Ontology functional categories of these genes were enriched in response to stress and defense against other organisms ($P < 0.001$). Notably, one-third of the genes significantly induced in both *35S:AnPGII* lines compared with the wild type encoded proteins putatively involved in cell wall structure and/or ROS homeostasis, including EXTENSIN4 (EXT4; At1g76930), a pectin esterase (At4g02330), copper/zinc superoxide dismutase1 (CSD1; At1g08830), and a CIII Prx (At5g64120).

At5g64120, which was among the genes whose expressions increased the most in *35S:AnPGII* plants (Table I), encodes the apoplastic CIII Prx ATP15a/AtPRX71, previously shown to produce ROS in response to hypoosmolarity (Rouet et al., 2006) and recently implicated in the regulation of stem lignin composition (Shigeto et al., 2013, 2015). *AtPRX71* is expressed under physiological conditions in rosette leaves and, to a lesser extent, roots and stems (Shigeto et al., 2015). Because we have previously observed high levels of ROS and apoplastic Prx activity in *35S:AnPGII* plants (Ferrari et al., 2008), we hypothesized that *AtPRX71* might contribute to the growth reduction observed in these plants by promoting ROS production. This gene was, therefore, selected for further characterization.

Higher levels of *AtPRX71* transcripts in rosette leaves of *35S:AnPGII* 57 plants compared with the wild type were confirmed by quantitative PCR (qPCR; Fig. 1A). Moreover, *AtPRX71* mRNA levels also increased in the *quasimodo2-1* (*qua2-1*) mutant (Fig. 1A), which is impaired in a putative pectin methyltransferase and, like *35S:AnPGII* plants, shows reduced levels of deesterified HG and impaired growth (Mouille et al., 2007). Moreover, *AtPRX71* transcript levels increased in wild-type Arabidopsis seedlings treated with the herbicide isoxaben (IXB; Fig. 1B), which inhibits cellulose synthases and affects cellulose deposition (Scheible et al., 2001). Taken together, these data indicate that alterations in different cell wall structural components promote the expression of *AtPRX71*.

AtPRX71 Negatively Regulates Arabidopsis Growth

To investigate the function of *AtPRX71*, two independent insertion lines for this gene were isolated; these lines, named *atprx71-1* and *atprx71-2*, carry a transfer DNA (T-DNA) insertion in the second exon and the promoter of the gene, respectively (Fig. 2, A and B). *AtPRX71* transcript levels were undetectable in *atprx71-1* and strongly reduced in *atprx71-2* seedlings (Fig. 2C). Basal guaiacol Prx activity, which characterizes CIII Prxs, was reduced in seedlings of both mutants by about 20%, compared with the wild type (Fig. 2D). Adult *atprx71-1* and *atprx71-2* plants displayed enhanced rosette size (Fig. 3A) and a significant increase in both fresh (Fig. 3B) and dry (Fig. 3C) biomass. An increase in biomass was also observed in 10-d-old mutant seedlings compared with the wild type (Fig. 3D). Hypocotyls of etiolated seedlings were significantly longer in both mutants than in the wild type (Fig. 3E), whereas average length and fresh weight of floral stems of wild-type and *atprx71-1* plants were not significantly different (Supplemental Fig. S1). These results indicated that *AtPRX71* negatively affects

Table I. *Genes differentially expressed in both 35S:AnPGII 57 and 26 plants compared with the wild type*

Differentially expressed transcripts were identified using Limma R package using an FDR < 0.05 and a module of logged FC on base 2 $|\log_2 FC| \geq 1.0$.

Arabidopsis Genome Initiative Code	Annotation	57[a]	26[a]
At1g77510	PROTEIN DISULFIDE ISOMERASE6	3.3	2.4
At1g76930	AtEXT4	2.8	3.0
At1g76960	Unknown protein	2.8	2.9
At5g64120	AtPRX71	2.7	2.7
At4g02330	PECTIN METHYLESTERASE41	2.4	1.6
At1g21520	Unknown protein	2.4	2.3
At1g08450	CALRETICULIN3	2.2	2.4
At5g50460	Protein transport protein SEC61 γ-subunit	2.1	1.9
At1g30720	RetOx-like flavin adenine dinucleotide-binding domain-containing protein	2.1	1.9
At4g21620	Gly-rich protein	1.8	1.8
At3g62600	ER-LOCALIZED DnaJ-LIKE PROTEIN 3b	1.7	1.4
At1g19380	Unknown protein	1.5	1.4
At1g08830	COPPER/ZINC SUPEROXIDE DISMUTASE1 (CSD1)	1.4	1.4
At2g38870	Ser-type endopeptidase inhibitor	1.4	2.2
At1g72070	DnaJ heat shock N-terminal domain-containing protein	1.3	1.5
At1g71697	CHOLINE KINASE1	1.3	1.7
At3g52500	Aspartyl protease	−2.1	−1.6
At3g47340	GLUTAMINE-DEPENDENT ASPARAGINE SYNTHASE1	−1.9	−1.6
At3g15570	NON-PHOTOTROPIC HYPOCOTYL3 family protein	−1.7	−1.4
At1g25550	MYB family transcription factor	−1.6	−1.7

[a]Log_2 FC of the expression in the transgenic line compared with the wild type.

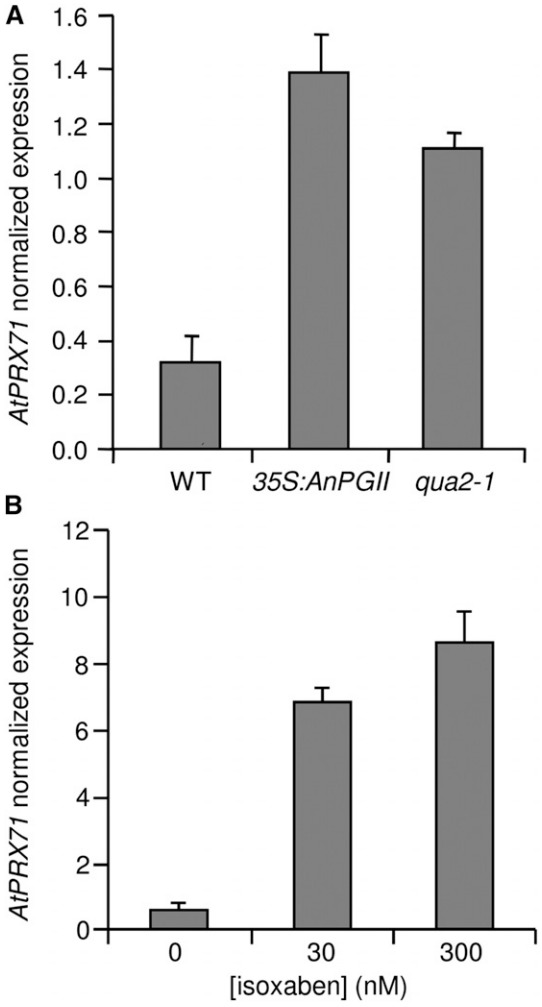

Figure 1. Elevated *AtPRX71* expression in plants with altered cell walls. Expression of *AtPRX71* in rosette leaves of 4-week-old wild-type (WT), *35S:AnPGII*, and *qua2-1* plants (A) or 10-d-old wild-type seedlings treated for 24 h with 0, 30, or 300 nM IXB (B) was determined by qPCR and normalized using the *UBQ5* gene. Bars represent average arbitrary units ± SD of three technical replicates. This experiment was repeated three times with similar results.

Arabidopsis growth. To corroborate this conclusion, we generated transgenic plants expressing *AtPRX71* under the control of the constitutive *Cauliflower mosaic virus* 35S promoter. Four independent *35S:AtPRX71* lines (21–24) accumulating high levels of *AtPRX71* transcripts (Fig. 4A) were selected for further analysis. When grown in soil, transgenic plants had smaller, more compact rosettes compared with the wild type (Fig. 4B). Lines 22 and 24, which showed higher expression of the transgene (Fig. 4A), exhibited a marked reduction of rosette size (Fig. 4B) and a significant reduction of rosette fresh weight (Fig. 4C). These lines also accumulated very high levels of guaiacol Prx activity in their leaves (Fig. 4D) compared with untransformed plants. Taken together, these data indicate that high levels of *AtPRX71* expression have a negative impact on plant growth. It has been proposed that CIII Prxs can restrict cell expansion by the formation of cell wall cross links (Passardi et al., 2004, 2005). We therefore hypothesized that the effects of AtPRX71 on Arabidopsis growth may depend on its ability to influence cell size. To verify this hypothesis, the area of the epidermal cells of rosette leaves was measured in wild-type, *atprx71-1*, *atprx71-2*, and *35S:AtPRX71* plants. Average cell area in both *atprx71* mutants increased by approximately 30% with respect to the wild type, whereas *35S:AtPRX71* plants showed a reduction of cell size of 20% to 30% (Fig. 5, A–F). These results, therefore, suggest that

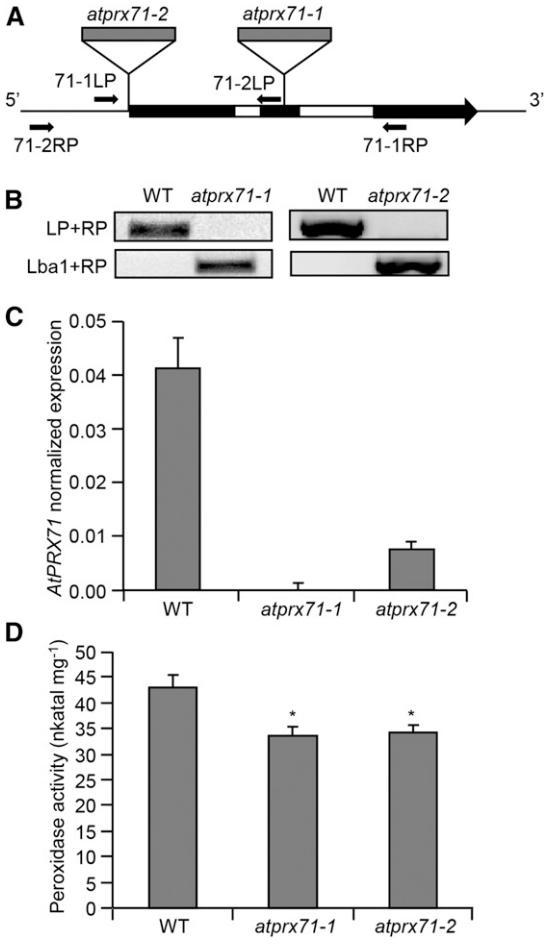

Figure 2. Isolation of insertional mutants for *AtPRX71*. A, Schematic representation of the *AtPRX71* locus. Exons and introns are represented in black and white, respectively. Localization of T-DNA insertions (gray) and the primers used for genotyping of *atprx71-1* and *atprx71-2* are shown. B, Genotyping of *atprx71-1* and *atprx71-2*. Genomic DNA from the wild type (WT) and mutants was subjected to PCR using primer pairs for the wild-type allele (LP + RP) or the T-DNA insertion (Lba1 + RP). LP, 71-1LP or 71-2LP; RP, 71-1RP or 71-2RP. C, Expression of *AtPRX71* was analyzed in wild-type, *atprx71-1*, and *atprx71-2* rosette leaves by qPCR using *UBQ5* as the reference gene. Bars represent average arbitrary units ± SD of three technical replicates. This experiment was repeated twice with similar results. D, Total peroxidase activity in protein extracts from wild-type, *atprx71-1*, and *atprx71-2* 10-d-old seedlings was determined by a guaiacol oxidation-based assay. Bars represent average activity ± SE of at least six independent samples. This experiment was repeated twice with similar results. *, Statistically significant differences between the wild type and mutants according to Student's *t* test ($P < 0.05$).

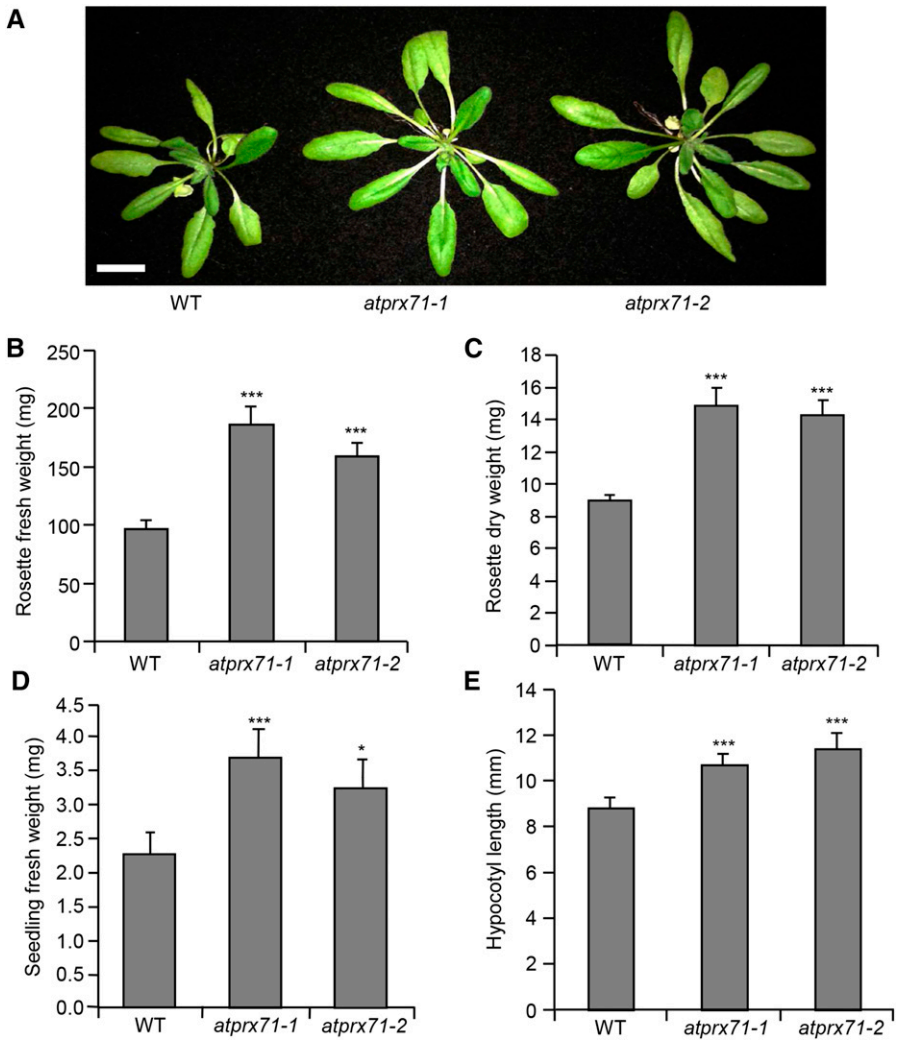

Figure 3. Loss of *AtPRX71* increases growth. A to C, Representative picture (A), fresh weight (B), and dry weight (C) of 4-week-old soil-grown wild-type (WT), *atprx71-1*, and *atprx71-2* rosettes. Bar =1.5 cm. D, Fresh weight of 10-d-old wild-type, *atprx71-1*, and *atprx71-2* seedlings grown in vitro on solid medium in the light. E, Hypocotyl length of 5-d-old wild-type, *atprx71-1*, and *atprx71-2* etiolated seedlings grown in vitro on solid medium. B to E, Bars represent average weight ± SE ($n > 10$ in each experiment); asterisks indicate statistically significant differences between the wild type and mutants according to Student's *t* test. *, $P < 0.05$; ***, $P < 0.01$.

AtPRX71 negatively regulates Arabidopsis growth, because its activity limits cell expansion.

To determine if the elevated levels of expression of *AtPRX71* contribute to the dwarf phenotype observed in plants with impaired CWI, we crossed *atprx71-1* and *35S*:*AnPGII* plants; however, expression of the transgene progressively declined in the subsequent generations, likely as a consequence of gene silencing, and homozygous F3 double-mutant plants did not show detectable PG activity (data not shown). For this reason, we crossed *atprx71-1* with *qua2-1* and analyzed the growth of homozygous double-mutant plants. Rosettes of soil-grown *atprx71-1 qua2-1* plants were bigger (Fig. 6A), and rosette fresh weight was almost 4 times greater (Fig. 6B) than in single *qua2-1* mutants. Hypocotyls of etiolated seedlings were also significantly longer in the double mutant compared with *qua2-1* seedlings (Fig. 6C). Total guaiacol peroxidase activity was higher in *qua2-1* plants than in the wild type at both seedling and adult stages, whereas activity in the *qua2-1 atprx71-1* double mutant was similar to that of the wild type, although not as low as in the *atprx71* mutants (Fig. 7). These data indicate that high levels of *AtPRX71* expression contribute to the dwarf phenotype of *qua2-1* plants, likely as a consequence of increased CIII Prx activity.

We also investigated whether AtPRX71 contributes to the growth defects caused by IXB treatment. Because this inhibitor strongly impairs Arabidopsis primary root elongation (Caño-Delgado et al., 2003; Tsang et al., 2011), we measured root length of wild-type, *atprx71-1*, and *atprx71-2* seedlings grown for 3 d in the presence of 2.5 and 10 nM IXB. In the absence of IXB, root length was comparable in all three genotypes (Fig. 8), indicating that AtPRX71 does not play a major role in regulating the growth of this organ. However, root elongation of *atprx71-1* and *atprx71-2* seedlings was less inhibited by IXB compared with the wild type (Fig. 8), suggesting that increased expression of *AtPRX71* triggered by the disruption of cellulose deposition contributes to restrict root growth. Transcript levels of two defense-related genes, *PHYTOALEXIN DEFICIENT3* (*PAD3*/*At3g26830*), encoding an enzyme catalyzing the biosynthesis of camalexin (Zhou et al., 1999), and *At1g26380* (*RetOx*), encoding a protein with homology to reticuline oxidases

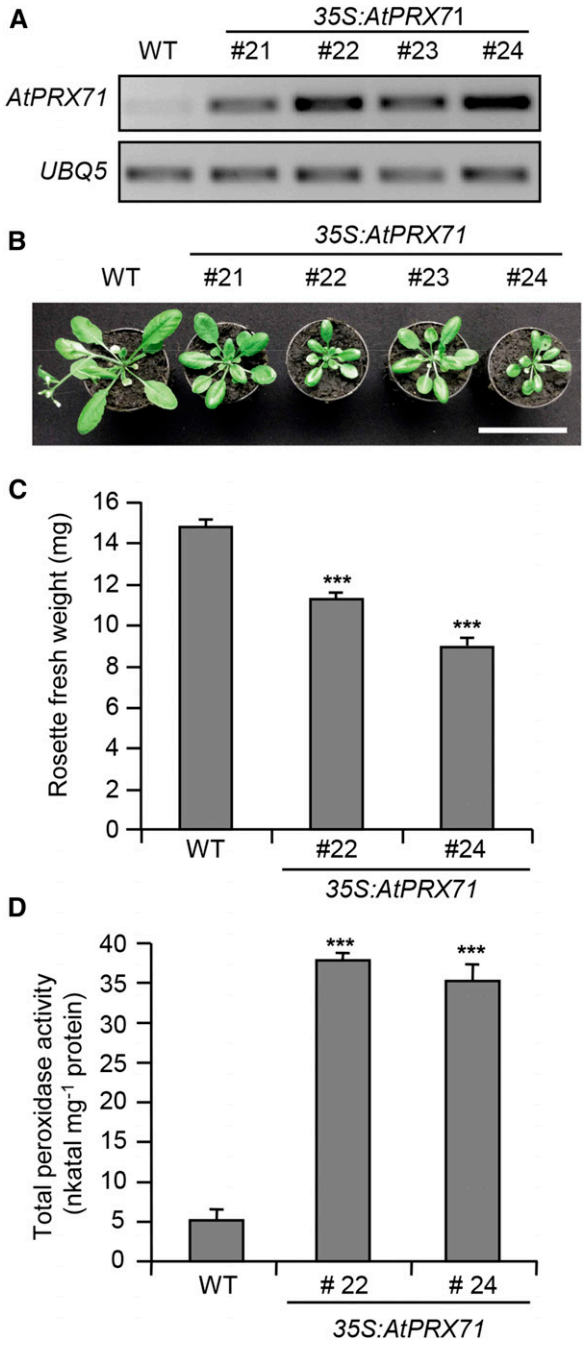

Figure 4. Overexpression of *AtPRX71* causes reduced growth. A, RNA was extracted from leaves of four-week-old wild-type (WT) plants and four independent lines expressing *AtPRX71* under the control of the 35S promoter (*35S:AtPRX71*). Expression of *AtPRX71* was determined by reverse transcription PCR using *UBQ5* as reference gene. B, Representative picture of rosettes of the same lines described in A. Bar = 5 cm. C, Average rosette fresh weight ± SE ($n > 10$) of the wild type and *35S:AtPRX71* lines 22 and 24 4-week-old soil-grown plants. D, Peroxidase activity in leaves of wild-type and *35S:AtPRX71* plants grown as in C. Bars represent average enzymatic activity (nanokatal milligram^{-1} protein) ± SD ($n = 3$). ***, Significant differences between wild-type and transgenic plants according to Student's *t* test ($P < 0.01$).

(Denoux et al., 2008), were also analyzed in wild-type, *atprx71-1*, and *atprx71-2* seedlings to determine whether *AtPRX71* is required also for IXB-induced gene expression. However, transcripts of both genes increased in response to IXB to a similar extent in wild-type and mutant plants (Supplemental Fig. S2). Therefore, partial resistance of *atprx71-1* and *atprx71-2* seedlings to IXB is likely not caused by an altered uptake or perception of the inhibitor. Taken together, these results lead to the conclusion that up-regulation of *AtPRX71* expression contributes to the reduced growth observed in plants undergoing loss of CWI.

AtPRX71 Promotes the Accumulation of ROS in Response to Cell Wall Alterations

Because CIII Prxs can inhibit cell expansion by promoting the accumulation of H_2O_2 in the apoplast (Lu

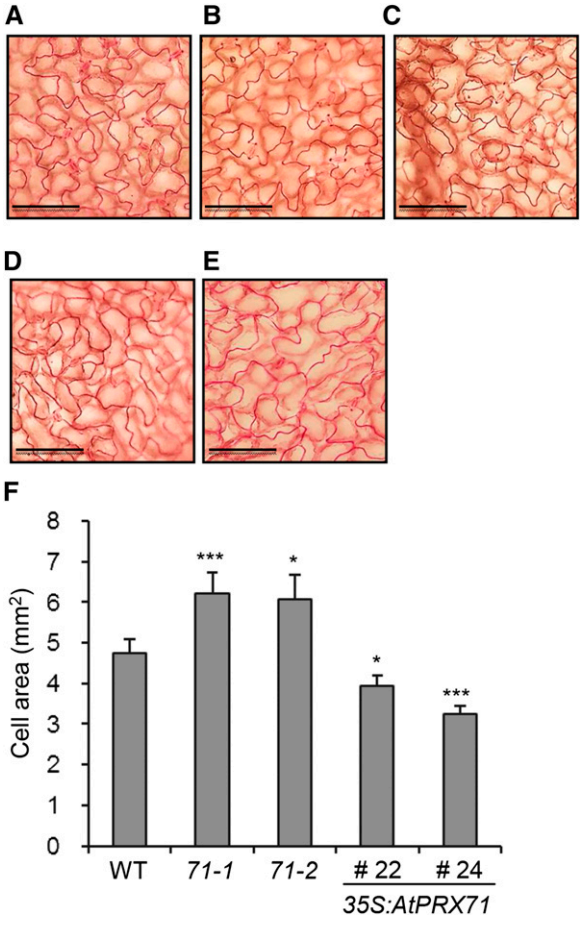

Figure 5. *AtPRX71* negatively affects leaf epidermal cell size. Rosette leaves from 3-week-old wild-type (WT; A), *atprx71-1* (B), and *atprx71-2* (C) plants and two lines overexpressing *AtPRX71* (*35S:AtPRX71* lines 22 [D] and 24 [E]) were cleared and stained with ruthenium red, and images of the epidermis were taken with a microscope. Bars = 100 μm. F, Bars represent the average area of epidermal cells ± SE ($n > 20$). Asterisks indicate significant differences between the wild type and mutants or transgenic plants according to Student's *t* test. *71-1*, *atprx71-2*; *71-2*, *atprx71-2*. *, $P < 0.05$; ***, $P < 0.01$.

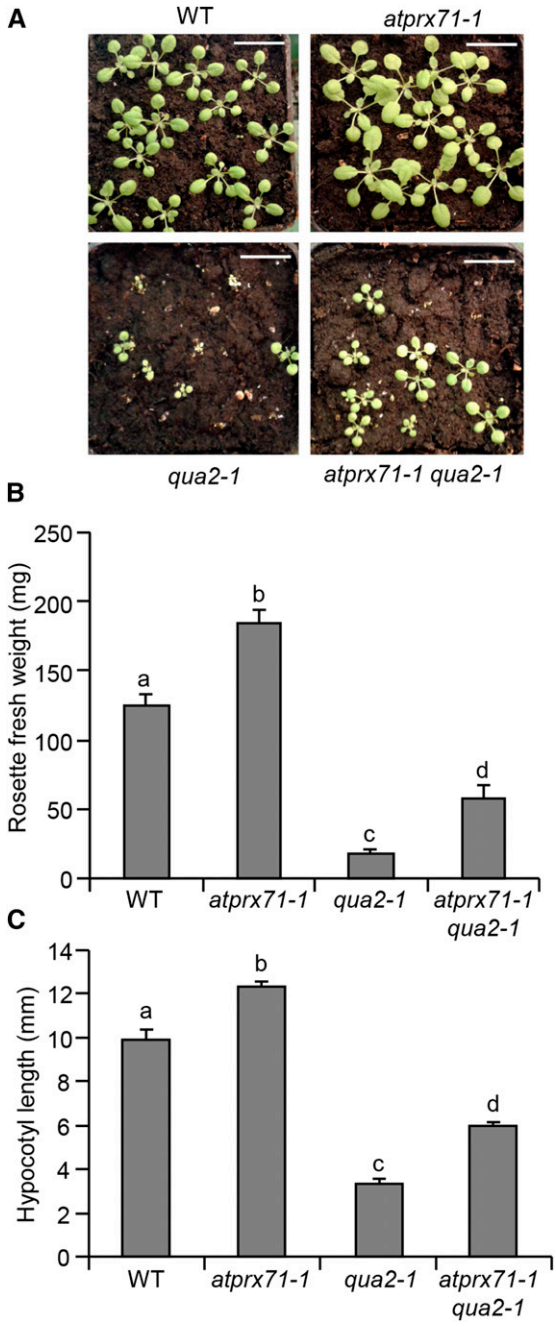

Figure 6. Loss of *AtPRX71* partially restores *qua2-1* growth defects. A, Representative picture of wild-type (WT), *atprx71-1*, *qua2-1*, and *atprx71-1 qua2-1* 3-week-old soil-grown rosettes. Bar = 1 cm. B, Rosette fresh weight of wild-type, *atprx71-1*, *qua2-1*, and *atprx71-1 qua2-1* 4-week-old soil-grown plants. Bars indicate average weight ± SE ($n > 10$). C, Hypocotyl length of 5-d-old wild-type, *atprx71-1*, and *atprx71-2* etiolated seedlings grown in vitro on solid medium ($n > 10$). Different letters in B and C indicate significant differences according to one-way ANOVA followed by Tukey's significance test ($P < 0.05$).

et al., 2014), we investigated whether high levels of *AtPRX71* expression are associated with increased ROS accumulation. Staining of leaves of *35S:AnPGII* plants with 3′,3′-diaminobenzidine (DAB) results in a strong brown coloration of the whole lamina, indicative of high levels of H_2O_2 and CIII Prxs (Ferrari et al., 2008). Here, we show that an intense DAB staining can also be observed in leaves of *qua2-1* plants (Fig. 9A), indicating that accumulation of high level of H_2O_2 is a common feature of plants with altered pectin. Notably, staining of rosette leaves was strongly reduced in leaves of the *atprx71-1 qua2-1* double mutant compared with *qua2-1* plants (Fig. 9A). This observation suggests that elevated levels of expression of *AtPRX71* are at least partially responsible for the accumulation of ROS caused by altered pectin composition. Consistently, leaves of *35S:AtPRX71* plants showed a strong DAB staining (Fig. 9B), supporting the conclusion that high levels of expression of *AtPRX71* promote the accumulation of ROS.

It has been reported that IXB induces the accumulation of H_2O_2 in Arabidopsis seedlings and that this accumulation is dependent on the NADPH oxidase AtrbohD (Denness et al., 2011). To determine whether AtPRX71 also contributes to this IXB-induced oxidative burst, wild-type and *atprx7-1* seedlings were treated with IXB using the *atrbohD* mutant as a negative control.

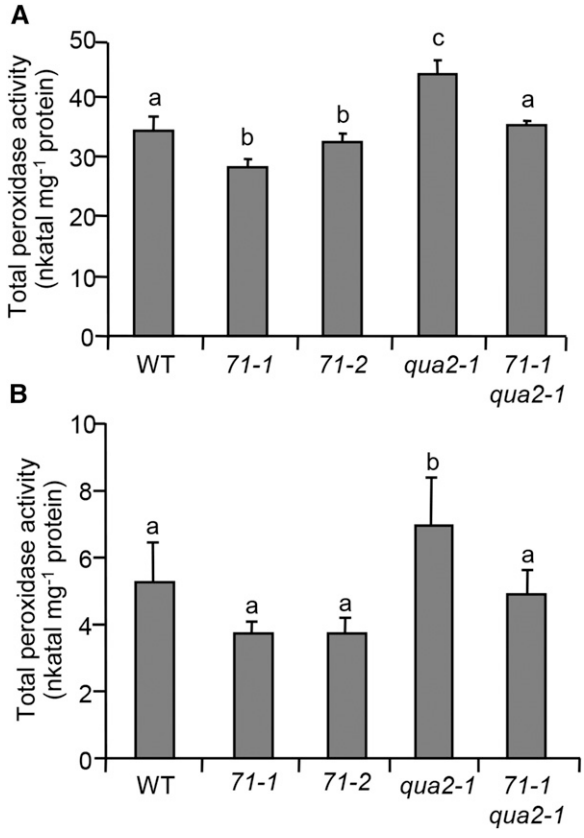

Figure 7. Peroxidase activity in *atprx71* and *qua2-1* mutants. Total proteins were extracted from 10-d-old in vitro-grown seedlings (A) or rosette leaves from 4-week-old soil-grown plants (B) and assayed for peroxidase activity. Bars represent average enzyme activity (nanokatal milligram^{-1} protein) ± SD ($n = 3$). Letters indicate significant differences according to one-way ANOVA followed by Tukey's significance test ($P < 0.05$). *71-1*, *atprx71-1*; *71-2*, *atprx71-2*; WT, wild type.

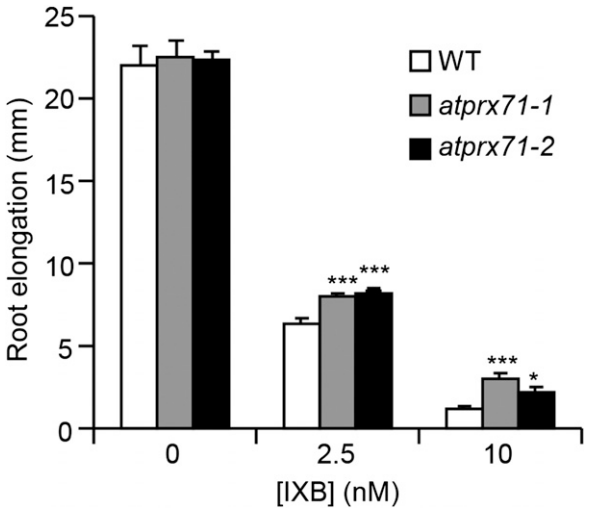

Figure 8. Inhibition of root elongation by IXB is partially reduced in *atprx71* mutants. Wild-type (WT), *atprx71-1*, and *atprx71-2* seedlings grown for 5 d on solid medium were transferred to solid medium containing the indicated doses of IXB. Primary root elongation was measured after 3 d. Bars indicate average elongation ± SE ($n > 12$). Asterisks indicate significant differences between the wild type and mutants according to Student's *t* test. This experiment was repeated twice with similar results. *, $P < 0.05$; ***, $P < 0.01$.

H_2O_2 started to accumulate in the wild type 3 to 4 h after treatment and steadily increased at least for the subsequent 14 to 15 h, whereas as expected, its accumulation was completely abolished in *atrbohD* seedlings (Fig. 9C). H_2O_2 production in *atprx71-1* and wild-type seedlings was comparable during the first 10 to 12 h of treatment, but then it increased much more slowly in the mutant, and after 18 h of treatment it was about one-half of that observed in the wild type (Fig. 9C). This observation leads to the conclusion that *AtPRX71* is not necessary for the initial onset of the IXB-induced oxidative burst, but it is required to ensure a sustained production of high levels of H_2O_2 in the apoplast. Taken together, these data indicate that *AtPRX71* contributes to the accumulation of ROS in plants with altered cell walls.

Production of ROS mediated by AtPRX71 may affect not only growth but also resistance to biotic stresses. Indeed, it was previously reported that Arabidopsis plants overexpressing *AtPRX71* show increased resistance to the fungus *Botrytis cinerea* (Chassot et al., 2007), suggesting that this CIII Prx can protect against pathogen infections. However, susceptibility of both *atprx71-1* and *atprx71-2* mutants to *B. cinerea* was comparable with that of the wild type (Supplemental Fig. S3), indicating that lack of *AtPRX71* alone is not sufficient to impair resistance to this fungus.

DISCUSSION

The plant cell wall is constantly subjected to modification and reorganization, both under physiological conditions and in response to abiotic and biotic stresses (Cheung and Wu, 2011). These changes allow cells to adapt their shape and size during development and in response to environmental stimuli. However, changes in cell wall composition can have detrimental effects, and plants, therefore, must constantly adjust cell walls

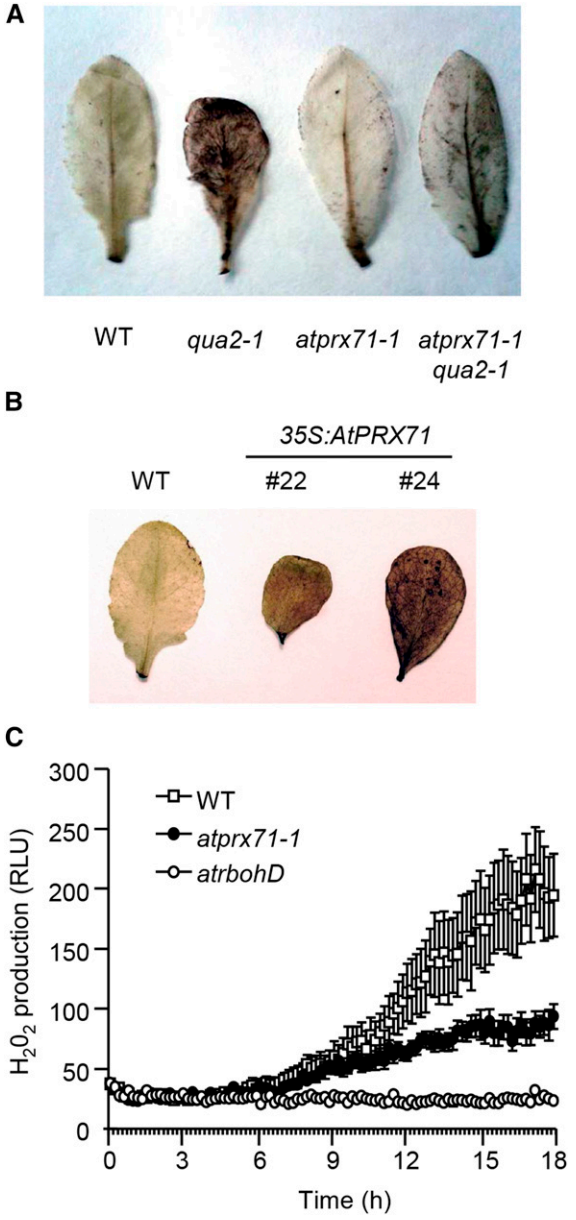

Figure 9. *AtPRX71* promotes ROS accumulation in response to cell wall modifications. ROS accumulation in rosette leaves of 4-week-old *qua2-1*, *atprx71-1*, and *atprx71-1 qua2-1* plants (A) and *35S:AtPRX71* plants belonging to lines 22 and 24 (B) was revealed by DAB staining. A representative picture for each genotype is shown. This experiment was repeated three (A) and two (B) times with similar results. C, Wild-type (WT), *atprx71-1*, and *atrbohD* seedlings grown for 3 d in liquid medium were treated with 600 nM IXB, and H_2O_2 production was measured every 10 min for 18 h with a luminol-based assay. Each point represents the average luminescence of 12 seedlings ± SD. This experiment was repeated three times with similar results. RLU, Relative luminescence unit.

to maintain their mechanical properties. Increasing evidence indicates that plants possess one or more mechanisms to perceive changes in the wall that may undermine its integrity and activate proper responses, including new structural modifications aimed at maintaining CWI (Hamann, 2012). CIII Prxs are likely among the effectors of this CWI maintenance system, contributing to strengthen the cell wall and, as a consequence, limiting cell expansion and plant growth. Indeed, CIII Prxs play important roles in the regulation of cell wall mechanical properties and cell expansion (Passardi et al., 2004, 2005). Here, we have shown that expression of an Arabidopsis gene encoding a CIII Prxs, namely *AtPRX71*, is elevated in plants with altered pectin composition (*35S*:*AnPGII* and *qua2-1* plants) or impaired in cellulose deposition (plants treated with IXB) and that lack of *AtPRX71* partially restores growth defects observed in these plants. Moreover, *AtPRX71* limits growth not only upon alterations of CWI but also under physiological conditions. Finally, AtPRX71 likely acts by promoting the accumulation of apoplastic ROS, which in turn may catalyze the formation of cross links, therefore stiffening the cell wall and restricting cell expansion.

The conclusion that *AtPRX71* encodes a CIII Prx that negatively affects growth is based on the observations that reduced expression of this gene leads to both reduced levels of peroxidase activity and increased rosette size and biomass, whereas *35S*:*AnPGII* plants show high levels of peroxidase activity and a significant reduction of biomass. Our findings are in agreement with previous reports describing other Arabidopsis CIII Prxs having negative effects on growth. For instance, overexpression of *AtPRX37* causes dwarfism (Pedreira et al., 2011), and plants mutated for or overexpressing *AtPRX53* exhibit longer or shorter hypocotyls, respectively (Jin et al., 2011). We also observed enhanced hypocotyl elongation in *atprx71-1* and *atprx71-2* etiolated seedlings; this latter result indicates that AtPRX71 regulates plant growth by restricting cell size rather than cell number, because it has been shown that elongation of etiolated hypocotyls occurs mainly by cell expansion (Gendreau et al., 1997). This conclusion is supported by the observation that, compared with the wild type, plants with reduced or increased levels of expression of *AtPRX71* display increased or decreased leaf epidermal cell size, respectively. Indeed, it has been recently reported that increased peroxidase activity is responsible for the defective cell expansion caused by the *kuoda1* mutant, which is impaired in a myeloblastosis oncoprotein (MYB)-like transcriptional repressor of different CIII Prx genes (Lu et al., 2014).

In addition to its role as a negative regulator of growth during normal development, *AtPRX71* seems to limit growth in plants with altered pectin composition, which was initially suggested by the elevated expression of this gene and the increased CIII Prx activity detected in *35S*:*AnPGII* plants (Ferrari et al., 2008) and *qua2-1* (this work) and subsequently, confirmed by the observation that the constitutively high peroxidase activity and the dwarf phenotype of *qua2-1* plants are partially reverted by the *atprx71-1* mutation. Furthermore, AtPRX71 seems to contribute to the growth defects caused by an altered cellulose deposition, because roots of *atprx71* seedlings are partially resistant to the inhibitory effect of IXB. Indeed, it has been previously shown that bean (*Phaseolus vulgaris*) cells habituated to dichlobenil, another inhibitor of cellulose synthesis, show increased guaiacol Prx activity (García-Angulo et al., 2009). It is, therefore, likely that accumulation of CIII Prxs is a conserved response of higher plants to cell wall damage.

The effects of AtPRX71 on Arabidopsis cell expansion and growth are likely mediated by its ability to promote the accumulation of apoplastic H_2O_2. Four lines of evidence support this hypothesis: (1) leaves of plants overexpressing *AtPRX71* accumulate high levels of ROS, (2) leaves of plants with altered pectin composition (*35S*:*AnPGII* plants and *qua2-1*) also accumulate high levels of ROS, (3) the *qua2-1 atprx71-1* double mutant shows reduced ROS accumulation compared with *qua2-1*, and (4) production of H_2O_2 in Arabidopsis seedlings treated with IXB is partially dependent on *AtPRX71*. ROS-mediated cross linking of wall structural components may be directly or indirectly catalyzed by AtPRX71 and, possibly, other CIII Prx isoforms to counteract cell wall damage. This mechanism may also act during normal development; indeed, ROS homeostasis controlled by CIII Prxs has been proposed to regulate leaf size in Arabidopsis (Lu et al., 2014). Notably, *AtPRX71* affects only the late phase of H_2O_2 production in response to IXB, indicating that this and possibly, other CIII Prxs may not be required for the initial onset of the oxidative burst triggered by cell wall damage, which is indeed dependent on NAPDH oxidases (Denness et al., 2011). However, CIII Prx may be necessary to maintain a robust and prolonged production of ROS for longer times after the initial burst is triggered.

The exact biochemical mechanism responsible for the effects of AtPRX71 on Arabidopsis growth still needs to be elucidated. *AtPRX71* has been implicated in stem lignification, although no alterations in stem lignin content but just a slight increase in the syringyl/guaiacyl lignin ratio was observed in knockout plants for this gene (Shigeto et al., 2013). Consistently, we did not detect significant differences in stem length and weight between wild-type and *atprx71* plants, confirming that *AtPRX71* has a negligible role in the lignification, at least in this organ. Characterization of AtPRX71 activity in vitro, however, indicates that this protein is able to oxidize 2,6-dimethoxyphenol and syringaldazine, which are model monolignol compounds (Shigeto et al., 2014), suggesting that this PRX may promote polymerization of lignin under specific conditions or in specific tissues. Moreover, AtPRX71 is also able to form protein radicals in vitro (Shigeto et al., 2014); the significantly increased expression of *EXT4* observed in *35S*:*AnPGII* plants, therefore, suggests that AtPRX71-mediated extensin cross links may be formed in response to altered CWI to strengthen the cell wall.

In addition to their role in plant growth, ROS-producing CIII Prxs have also been implicated in defense against pathogens. In Arabidopsis, AtPRX33 and AtPRX34 contribute to a significant proportion of the H_2O_2 generated in response to microbe-associated molecular patterns and are required for resistance to different pathogens and for the activation of some defense responses (Bindschedler et al., 2006; Daudi et al., 2012; O'Brien et al., 2012) and in particular, salicylic acid-mediated gene expression (Mammarella et al., 2015). ROS generated by AtPRX33 and AtPRX34 during infection can therefore participate in Arabidopsis defense not only by promoting cell wall reinforcement but also indirectly through the modulation of the immune response. Additional CIII Prx isoforms, including AtPRX71, that are able to favor the accumulation of ROS in the apoplast, may also contribute to Arabidopsis resistance against microbes. Indeed, it was previously shown that overexpression of *AtPRX71* as well as two other CIII Prx genes confers strong resistance to *B. cinerea* infection (Chassot et al., 2007). However, *AtPRX71* is dispensable for basal resistance to this pathogen, because *atprx71-1* and *atprx71-2* plants show wild-type susceptibility (this work). This apparent incongruence can be explained if expression of multiple CIII Prxs is induced during infection, acting redundantly to promote ROS production and resistance to microbes. If this is the case, lack of a single isoform would not significantly decrease the plant ability to limit pathogen growth; however, overexpression of any of these Prxs would be sufficient to boost accumulation of ROS, which we have observed in the case of *35S:AtPRX71* plants, therefore conferring a strong resistant phenotype.

The results presented in this work indicate that modifications of different cell wall structural components increase the expression of *AtPRX71*, which in turns, leads to ROS production and cell wall reinforcement. This implies that CWI perturbations may activate common responses, regardless of the specific component that is affected. For example, alterations of different structural polysaccharides would result in cell wall weakening, which may be perceived through the stretching of the plasma membrane under the effect of turgor pressure (Hamann, 2012). Mechanosensitive channels may thus be activated and trigger downstream responses, including accumulation of CIII Prxs. This model is supported by the observation that some phenotypes induced by IXB, such as ectopic deposition of lignin, can be reverted by osmotic support (Hamann et al., 2009). Moreover, hypoosmotic stress alone can lead to AtPRX71-mediated production of ROS (Rouet et al., 2006), suggesting that changes in turgor pressure can directly induce the expression of this peroxidase. Alternatively, loss of CWI may result in the release of elicitor-active cell wall fragments, which may be responsible for the induction of *AtPRX71* expression. For instance, oligogalacturonides produced by partial degradation of HG trigger the activation of several defense responses in Arabidopsis (Ferrari et al., 2013; Benedetti et al., 2015), including the expression of *AtPRX71* (Ferrari et al., 2007; Denoux et al., 2008). Further studies are required to discriminate between these two hypotheses, which are not, however, mutually exclusive.

Other than providing unique insights into the biological mechanisms regulating plant growth, our findings can be relevant to improve crops dedicated to the production of biofuels and other industrial products. Increasing evidence supports the idea that targeted modifications of cell wall structural components can increase the efficiency of conversion of lignocellulosic biomasses (Chen and Dixon, 2007; Kaida et al., 2009; Selig et al., 2009; Lionetti et al., 2010). Knowledge about how to manipulate cell wall composition without detrimental effects on growth and resistance to stresses is, therefore, needed. We have previously shown that *35S:AnPGII* and *qua2-1* plants are more efficiently degraded by cellulase (Lionetti et al., 2010; Francocci et al., 2013), indicating that pectin composition strongly affects biomass utilization. However, a major reduction in HG content severely impairs growth, strongly limiting the application of this approach. According to the results presented here, the detrimental effects of pectin modification on growth might be avoided by reducing the expression of specific CIII Prx isoforms. Notably, we found that lack of *AtPRX71* increases biomass production without negative effects on resistance to pathogens, at least in the case of *B. cinerea*. Because CIII Prxs also negatively regulate saccharification efficiency (Kavousi et al., 2010), crops with both targeted modifications of cell wall composition and reduced levels of selected CIII Prxs may be more efficiently processed without detrimental effects or even a positive impact on biomass production.

In conclusion, our results indicate that wall stiffening and the consequent inhibition of growth mediated by CIII Prxs like AtPRX71 may be an important component of CWI maintenance (Hamann, 2012), both during physiological developmental processes (e.g. expansion of new organs) and in response to stresses (e.g. wounding or pathogen attack). These findings provide unique insights into the mechanisms of regulation of plant growth and may be used in the development of crop varieties with improved biomass production and utilization.

MATERIALS AND METHODS

Biological Material and Growth Conditions

All Arabidopsis (*Arabidopsis thaliana*) plants used in this work are in the Columbia-0 (Col-0) background. Wild-type Col-0 seeds were obtained from Lehle Seeds. The insertion lines *atprx71-1* (SALK_123643) and *atprx71-2* (SALK_121202C) were obtained from the Salk Institute Genomic Analysis Laboratory (Alonso et al., 2003). The generation of Col-0 plants expressing the *Aspergillus niger PGII* gene (*35S:AnPGII* plants; lines 26 and 57) and the isolation and characterization of the *qua2-1* mutant have been previously described (Mouille et al., 2007; Lionetti et al., 2010).

Plants were grown in soil (Einheitserde) in a growth chamber at 22°C and 70% relative humidity with a 16-h-light/8-h-dark photoperiod using fluorescent lamps (Osram). Light intensity was about 120 μmol m^{-2} s^{-1}. Before sowing, seeds were always stratified in sterile water for 3 d in the dark at +4°C.

For in vitro growth, seeds were surface sterilized as previously described (Ferrari et al., 2007) and stratified as described above. For growth on solid medium, seeds were germinated on plates containing one-half-strength Murashige and Skoog medium (MS; Murashige and Skoog, 1962) basal salts supplemented with 1% (w/v) Suc unless otherwise stated and 0.7% (w/v) plant

agar, pH 5.0. For analysis of gene expression after IXB treatments, sterilized seeds were distributed in 12-well plates (about 10 seeds per well) containing 1 mL of 2.2 g L^{-1} basal MS supplemented with 0.5% (w/v) Suc, pH 5.5. After 9 d, the medium was replaced with fresh medium, and after 1 d, seedlings were treated for 24 h with filter-sterilized 0.01% (v/v) dimethyl sulfoxide or IXB (Sigma) at the indicated concentrations.

Gene Expression Analysis

Leaves or seedlings were frozen in liquid nitrogen and homogenized with an MM301 Ball Mill (Retsch) for about 2 min at 30 Hz. Total RNA was extracted with Isol-RNA Lysis Reagent (5′-Prime) according to the manufacturer's instructions.

Full-genome transcriptome analysis was performed on custom Arabidopsis 28K v2.0 Microarrays (GenBank GEO Platform ID no. GPL15543) synthesized using a CombiMatrix B3 Synthesizer (Combimatrix) according to manufacturer's instructions. Total RNA (1 μg) was amplified, and 6 μg of antisense RNA was labeled using the RNA AmpULSe Amplification and Labeling Kit with Cy5 for CombiMatrix Arrays (Kreatech Biotechnology) according to the manufacturer's instructions. Labeled samples were hybridized to the microarrays according to CombiMatrix protocols. Scanning was performed on a GenePix 4000B Scanner (Molecular Devices). Data extraction was done using Microarray Imager software (Combimatrix), and quantile normalization of data was performed using Blist v0.6 software (Combimatrix). Differentially expressed transcripts were identified using Limma R package using an FDR < 0.05 and a module of logged FC on base 2 $|\log_2 FC| \geq 1$ (Smyth, 2004). Expression data are available from the National Center for Biotechnology Information (GEO accession no. GSE66980). Gene Ontology categories enrichment of differentially expressed genes was determined with the aid of the AgriGO Toolkit (Du et al., 2010).

For reverse transcription PCR analysis, RNA was treated with RQ1 DNase (Promega), and first-strand complementary DNA was obtained using Improm II Reverse Transcriptase (Promega). PCR was performed using Taq DNA Polymerase (RBC-Bioscience) with primers specific for the genes of interest (Supplemental Table S1) using the following conditions: 94°C for 2 min; 28 cycles as follows: 30 s at 94°C, 30 s at 58°C, and 30 s at 72°C; and 72°C for 5 min. Real-time PCR was performed using a CFX96 Real-Time System (Bio-Rad). Complementary DNA (corresponding to 50 ng of total RNA) was amplified using GoTaq qPCR Master Mix (Promega) and 0.4 mM each primer. Expression levels of each gene, relative to *UBIQUITIN5* (*UBQ5*) were determined using a modification of the method by Pfaffl (2001)) as previously described (Ferrari et al., 2006).

Plant Growth Measurement

Rosette fresh weight was measured in 4-week-old soil-grown plants. Dry weight measurements were performed on the same material after incubation for 8 h at 60°C. Fresh weight of seedlings was determined after 10 d of growth in solid MS.

For measurements of hypocotyls in etiolated seedlings, sterilized seeds were sown on solid MS containing 1% (w/v) plant agar. Plates were incubated for 4 h under constant light at 25°C, wrapped with aluminum foil, and transferred to a growth chamber. Hypocotyl length was measured after incubation in the dark at 22°C for 5 d.

For cell area determination, the fifth leaf of 3-week-old soil-grown plants (at least four plants for genotype) was harvested, and chlorophyll was extracted in 100% boiling ethanol. Cleared leaves were stained with 0.05% (w/v) ruthenium red. Excess dye was removed by washing leaves with water. Leaves were mounted in 20% (v/v) glycerol and examined using a Nikon Eclipse E200 Microscope. Images were taken with a Nikon Digital Sight DS-Fi1c Camera, and cell area was measured using ImageJ (http://rsbweb.nih.gov/ij/index.html).

Fungal Infections

Growth of *Botrytis cinerea* and inoculation of Arabidopsis leaves were conducted as previously described (Ferrari et al., 2003).

Isolation and Genotyping of Mutants

Genomic DNA was extracted from 4-week-old plants using the method by Edwards et al. (1991). Genomic DNA was subjected to PCR to detect the wild-type allele of *AtPRX71* using 71-1RP and 71-1LP primers (Supplemental Table S1) for *atprx71-1* and 71-2RP and 71-2LP for *atprx71-2*. To detect the insertion of the T-DNA, the Lba1 primer (Supplemental Table S1) was used in place of the LP primer. Samples were subjected to amplification using Taq DNA Polymerase (RCB-Bioscience) under the following conditions: 2 min at 94°C; 35 cycles as follows: 30 s at 94°C, 30 s at 60°C, and 45 s at 72°C; and 7 min at 72°C. PCR products were separated by agarose gel electrophoresis and visualized by ethidium bromide staining.

Generation of double *atprx71-1 qua2-1* mutants was achieved by crossing of single-mutant plants. F2 individuals were screened for the *atprx71-1* mutation as described above, whereas the *qua2-1* mutation was detected by high-resolution DNA melting analysis (Vossen et al., 2009). Briefly, genomic DNA was amplified by real-time PCR as described above with the QUA2FW and QUA2REV primers (Supplemental Table S1) using an annealing temperature of 59°C. Melting curves of the PCR products from 70°C to 80°C were obtained using 0.2°C increments in temperature at each fluorescence measurement step.

Generation of Plants Overexpressing *AtPRX71*

The *AtPRX71* genomic region, starting from the predicted translation start codon and ending in correspondence of the predicted translation stop codon, was amplified using Col-0 genomic DNA as a template. PCR was performed with High-Fidelity PCR Master Mix (Roche) using the OEXPOX1FW and OEXPOX1-REV primers (Supplemental Table S1). The purified PCR fragment was cloned into the pGEM T-Easy Vector (Promega), and the obtained plasmid was introduced in *Escherichia coli* DH5α by electroporation. The insert was excised from the plasmid using *Xba*I and *Sac*I (Fermentas), gel purified, and subcloned into the binary vector pBI121 (Stratagene) in place of the beta-glucuronidase *uidA* gene. After ligation and electroporation into *E. coli* DH5α cells, the obtained plasmid (pBI121-AtPRX71), which contains the *AtPRX71* gene under the control of the *Cauliflower mosaic virus* 35S promoter, was introduced in *Agrobacterium tumefaciens* GV3101 cells. Arabidopsis Col-0 plants were transformed with the obtained bacterial strain using the floral dip method (Clough and Bent, 1998). Transformants were selected on solid MS plates supplemented with 50 μg mL^{-1} kanamycin.

Oxidative Burst Assay

For determination of the oxidative burst elicited by IXB, a luminol-based protocol (Denness et al., 2011) was used. Arabidopsis seedlings were grown in sterile 96-well plates (Costar) on Gamborg's medium supplemented with 1% (w/v) Suc, pH 5.5, for 6 d at 23°C. Before the experiment, the medium was removed, and 100 μL of assay solution (17 mM luminol [Sigma], 1 μM horseradish PRX [Sigma], and 600 nM IXB) was added to each well. Plates were placed in a GloMax 96 Microplate Luminometer (Promega), and luminescence was measured for 18 h at 10-min intervals using an integration time of 1 s.

Histochemical Analyses

For H_2O_2 visualization, rosette leaves from 4-week-old plants were incubated for 12 h in a solution containing 1 mg mL^{-1} DAB, pH 5.0. Chlorophyll was extracted for 10 min with boiling ethanol and 2 h with ethanol at room temperature before photography (Orozco-Cardenas and Ryan, 1999).

Measurement of CIII Prx Activity

Soluble proteins were extracted from 10-d-old seedlings and 4-week-old rosette leaves by grinding in the following extraction buffer (1 mL for 100 mg of seedlings and 50 μL for 100 mg of leaves): 20 mM HEPES, pH 7.0, 1 mM EGTA, 10 mM vitamin C, and PVP PolyclarAT (100 mg g^{-1} fresh weight). The extract was centrifuged two times (10 min at 10,000*g* and 4°C) to remove insoluble material. Subsequent experiments were carried out on the supernatant. The protein content was determined using the Bradford Reagent (Serva) with bovine serum albumin (Sigma-Aldrich) as a standard (Bradford, 1976). PRX activity was measured at 25°C by following the oxidation of 8 mM guaiacol (Fluka) at 470 nm in the presence of 2 mM H_2O_2 (Carlo Erba) in a phosphate buffer (200 mM, pH 6.0).

Sequence data from this article are as follows: *At5g64120* (*AtPRX71*), *At3g62250* (*UBQ5*), *At3g26830* (*PAD3*), and *At1g26380* (*RetOx*).

Supplemental Data

The following supplemental materials are available.

Supplemental Figure S1. Lack of *AtPRX71* does not affect stem growth.

Supplemental Figure S2. Gene expression induced by IXB is not altered in *atprx71* plants.

Supplemental Figure S3. *AtPRX71* is not required for basal resistance to *B. cinerea*.

Supplemental Table S1. Primers used in this work.

ACKNOWLEDGMENTS

We thank Dr. Grégory Mouille and Stéphane Verger (Institut National de la Recherche Agronomique, Centre de Recherche de Versailles-Grignon, France) for providing *qua2-1* seeds and assistance in the genotyping of this mutant.

Received September 15, 2015; accepted October 13, 2015; published October 14, 2015.

LITERATURE CITED

Alonso JM, Stepanova AN, Leisse TJ, Kim CJ, Chen H, Shinn P, Stevenson DK, Zimmerman J, Barajas P, Cheuk R, et al (2003) Genome-wide insertional mutagenesis of *Arabidopsis thaliana*. Science **301:** 653–657

Benedetti M, Pontiggia D, Raggi S, Cheng Z, Scaloni F, Ferrari S, Ausubel FM, Cervone F, De Lorenzo G (2015) Plant immunity triggered by engineered in vivo release of oligogalacturonides, damage-associated molecular patterns. Proc Natl Acad Sci USA **112:** 5533–5538

Bindschedler LV, Dewdney J, Blee KA, Stone JM, Asai T, Plotnikov J, Denoux C, Hayes T, Gerrish C, Davies DR, et al (2006) Peroxidase-dependent apoplastic oxidative burst in Arabidopsis required for pathogen resistance. Plant J **47:** 851–863

Bolwell GP, Blee KA, Butt VS, Davies DR, Gardner SL, Gerrish C, Minibayeva F, Rowntree EG, Wojtaszek P (1999) Recent advances in understanding the origin of the apoplastic oxidative burst in plant cells. Free Radic Res (Suppl) **31:** S137–S145

Bradford MM (1976) A rapid and sensitive method for the quantitation of microgram quantities of protein utilizing the principle of protein-dye binding. Anal Biochem **72:** 248–254

Caffall KH, Mohnen D (2009) The structure, function, and biosynthesis of plant cell wall pectic polysaccharides. Carbohydr Res **344:** 1879–1900

Caño-Delgado A, Penfield S, Smith C, Catley M, Bevan M (2003) Reduced cellulose synthesis invokes lignification and defense responses in Arabidopsis thaliana. Plant J **34:** 351–362

Capodicasa C, Vairo D, Zabotina O, McCartney L, Caprari C, Mattei B, Manfredini C, Aracri B, Benen J, Knox JP, et al (2004) Targeted modification of homogalacturonan by transgenic expression of a fungal polygalacturonase alters plant growth. Plant Physiol **135:** 1294–1304

Carpita N, McCann M (2000) The cell wall. *In* BB Buchanan, W Gruissem, RL Jones, eds, Biochemistry and Molecular Biology of Plants. American Society of Plant Physiologists, Rockville, MD, pp 52–108

Chassot C, Nawrath C, Métraux JP (2007) Cuticular defects lead to full immunity to a major plant pathogen. Plant J **49:** 972–980

Chen F, Dixon RA (2007) Lignin modification improves fermentable sugar yields for biofuel production. Nat Biotechnol **25:** 759–761

Chen SX, Schopfer P (1999) Hydroxyl-radical production in physiological reactions. A novel function of peroxidase. Eur J Biochem **260:** 726–735

Cheung AY, Wu HM (2011) THESEUS 1, FERONIA and relatives: a family of cell wall-sensing receptor kinases? Curr Opin Plant Biol **14:** 632–641

Clough SJ, Bent AF (1998) Floral dip: a simplified method for *Agrobacterium*-mediated transformation of *Arabidopsis thaliana*. Plant J **16:** 735–743

Cosgrove DJ (2000) Expansive growth of plant cell walls. Plant Physiol Biochem **38:** 109–124

Cosio C, Dunand C (2009) Specific functions of individual class III peroxidase genes. J Exp Bot **60:** 391–408

Crowell EF, Gonneau M, Vernhettes S, Höfte H (2010) Regulation of anisotropic cell expansion in higher plants. C R Biol **333:** 320–324

Daudi A, Cheng Z, O'Brien JA, Mammarella N, Khan S, Ausubel FM, Bolwell GP (2012) The apoplastic oxidative burst peroxidase in *Arabidopsis* is a major component of pattern-triggered immunity. Plant Cell **24:** 275–287

Denness L, McKenna JF, Segonzac C, Wormit A, Madhou P, Bennett M, Mansfield J, Zipfel C, Hamann T (2011) Cell wall damage-induced lignin biosynthesis is regulated by a reactive oxygen species- and jasmonic acid-dependent process in Arabidopsis. Plant Physiol **156:** 1364–1374

Denoux C, Galletti R, Mammarella N, Gopalan S, Werck D, De Lorenzo G, Ferrari S, Ausubel FM, Dewdney J (2008) Activation of defense response pathways by OGs and Flg22 elicitors in Arabidopsis seedlings. Mol Plant **1:** 423–445

Du Z, Zhou X, Ling Y, Zhang Z, Su Z (2010) agriGO: a GO analysis toolkit for the agricultural community. Nucleic Acids Res **38:** W64–W70

Dunand C, de Meyer M, Crevecoeur M, Penel C (2003) Expression of a peroxidase gene in zucchini in relation with hypocotyl growth. Plant Physiol Biochem **41:** 805–811

Edwards K, Johnstone C, Thompson C (1991) A simple and rapid method for the preparation of plant genomic DNA for PCR analysis. Nucleic Acids Res **19:** 1349

Ferrari S, Galletti R, Denoux C, De Lorenzo G, Ausubel FM, Dewdney J (2007) Resistance to *Botrytis cinerea* induced in Arabidopsis by elicitors is independent of salicylic acid, ethylene, or jasmonate signaling but requires PHYTOALEXIN DEFICIENT3. Plant Physiol **144:** 367–379

Ferrari S, Galletti R, Pontiggia D, Manfredini C, Lionetti V, Bellincampi D, Cervone F, De Lorenzo G (2008) Transgenic expression of a fungal *endo*-polygalacturonase increases plant resistance to pathogens and reduces auxin sensitivity. Plant Physiol **146:** 669–681

Ferrari S, Galletti R, Vairo D, Cervone F, De Lorenzo G (2006) Antisense expression of the *Arabidopsis thaliana AtPGIP1* gene reduces polygalacturonase-inhibiting protein accumulation and enhances susceptibility to *Botrytis cinerea*. Mol Plant Microbe Interact **19:** 931–936

Ferrari S, Plotnikova JM, De Lorenzo G, Ausubel FM (2003) Arabidopsis local resistance to *Botrytis cinerea* involves salicylic acid and camalexin and requires EDS4 and PAD2, but not SID2, EDS5 or PAD4. Plant J **35:** 193–205

Ferrari S, Savatin DV, Sicilia F, Gramegna G, Cervone F, Lorenzo GD (2013) Oligogalacturonides: plant damage-associated molecular patterns and regulators of growth and development. Front Plant Sci **4:** 49

Francocci F, Bastianelli E, Lionetti V, Ferrari S, De Lorenzo G, Bellincampi D, Cervone F (2013) Analysis of pectin mutants and natural accessions of Arabidopsis highlights the impact of de-methyl-esterified homogalacturonan on tissue saccharification. Biotechnol Biofuels **6:** 163

Fry SC, Smith RC, Renwick KF, Martin DJ, Hodge SK, Matthews KJ (1992) Xyloglucan endotransglycosylase, a new wall-loosening enzyme activity from plants. Biochem J **282:** 821–828

Gapper C, Dolan L (2006) Control of plant development by reactive oxygen species. Plant Physiol **141:** 341–345

García-Angulo P, Alonso-Simón A, Mélida H, Encina A, Acebes JL, Alvarez JM (2009) High peroxidase activity and stable changes in the cell wall are related to dichlobenil tolerance. J Plant Physiol **166:** 1229–1240

Gendreau E, Traas J, Desnos T, Grandjean O, Caboche M, Höfte H (1997) Cellular basis of hypocotyl growth in *Arabidopsis thaliana*. Plant Physiol **114:** 295–305

Hamann T (2012) Plant cell wall integrity maintenance as an essential component of biotic stress response mechanisms. Front Plant Sci **3:** 77

Hamann T, Bennett M, Mansfield J, Somerville C (2009) Identification of cell-wall stress as a hexose-dependent and osmosensitive regulator of plant responses. Plant J **57:** 1015–1026

Hiraga S, Sasaki K, Ito H, Ohashi Y, Matsui H (2001) A large family of class III plant peroxidases. Plant Cell Physiol **42:** 462–468

Iiyama K, Lam T, Stone BA (1994) Covalent cross-links in the cell wall. Plant Physiol **104:** 315–320

Jin J, Hewezi T, Baum TJ (2011) Arabidopsis peroxidase AtPRX53 influences cell elongation and susceptibility to *Heterodera schachtii*. Plant Signal Behav **6:** 1778–1786

Kaida R, Kaku T, Baba K, Oyadomari M, Watanabe T, Nishida K, Kanaya T, Shani Z, Shoseyov O, Hayashi T (2009) Loosening xyloglucan accelerates the enzymatic degradation of cellulose in wood. Mol Plant **2:** 904–909

Kavousi B, Daudi A, Cook CM, Joseleau JP, Ruel K, Devoto A, Bolwell GP, Blee KA (2010) Consequences of antisense down-regulation of a lignification-specific peroxidase on leaf and vascular tissue in tobacco lines demonstrating enhanced enzymic saccharification. Phytochemistry **71:** 531–542

Keegstra K (2010) Plant cell walls. Plant Physiol **154:** 483–486

Lionetti V, Francocci F, Ferrari S, Volpi C, Bellincampi D, Galletti R, D'Ovidio R, De Lorenzo G, Cervone F (2010) Engineering the cell wall by reducing de-methyl-esterified homogalacturonan improves saccharification of plant tissues for bioconversion. Proc Natl Acad Sci USA **107:** 616–621

Lu D, Wang T, Persson S, Mueller-Roeber B, Schippers JH (2014) Transcriptional control of ROS homeostasis by KUODA1 regulates cell expansion during leaf development. Nat Commun **5:** 3767

Mammarella ND, Cheng Z, Fu ZQ, Daudi A, Bolwell GP, Dong X, Ausubel FM (2015) Apoplastic peroxidases are required for salicylic acid-mediated defense against *Pseudomonas syringae*. Phytochemistry **112:** 110–121

Marjamaa K, Kukkola EM, Fagerstedt KV (2009) The role of xylem class III peroxidases in lignification. J Exp Bot **60:** 367–376

Micheli F (2001) Pectin methylesterases: cell wall enzymes with important roles in plant physiology. Trends Plant Sci **6:** 414–419

Mirabet V, Das P, Boudaoud A, Hamant O (2011) The role of mechanical forces in plant morphogenesis. Annu Rev Plant Biol **62:** 365–385

Mouille G, Ralet MC, Cavelier C, Eland C, Effroy D, Hématy K, McCartney L, Truong HN, Gaudon V, Thibault JF, et al (2007) Homogalacturonan synthesis in Arabidopsis thaliana requires a Golgi-localized protein with a putative methyltransferase domain. Plant J **50:** 605–614

Murashige T, Skoog F (1962) Revised medium for rapid growth and bioassays with tobacco cultures. Physiol Plant **15:** 437–479

O'Brien JA, Daudi A, Finch P, Butt VS, Whitelegge JP, Souda P, Ausubel FM, Bolwell GP (2012) A peroxidase-dependent apoplastic oxidative burst in cultured Arabidopsis cells functions in MAMP-elicited defense. Plant Physiol **158:** 2013–2027

Orozco-Cardenas M, Ryan CA (1999) Hydrogen peroxide is generated systemically in plant leaves by wounding and systemin via the octadecanoid pathway. Proc Natl Acad Sci USA **96:** 6553–6557

Passardi F, Cosio C, Penel C, Dunand C (2005) Peroxidases have more functions than a Swiss army knife. Plant Cell Rep **24:** 255–265

Passardi F, Penel C, Dunand C (2004) Performing the paradoxical: how plant peroxidases modify the cell wall. Trends Plant Sci **9:** 534–540

Pedreira J, Herrera MT, Zarra I, Revilla G (2011) The overexpression of AtPrx37, an apoplastic peroxidase, reduces growth in Arabidopsis. Physiol Plant **141:** 177–187

Pelloux J, Rustérucci C, Mellerowicz EJ (2007) New insights into pectin methylesterase structure and function. Trends Plant Sci **12:** 267–277

Pfaffl MW (2001) A new mathematical model for relative quantification in real-time RT-PCR. Nucleic Acids Res **29:** e45

Rouet MA, Mathieu Y, Barbier-Brygoo H, Laurière C (2006) Characterization of active oxygen-producing proteins in response to hypo-osmolarity in tobacco and Arabidopsis cell suspensions: identification of a cell wall peroxidase. J Exp Bot **57:** 1323–1332

Scheible WR, Eshed R, Richmond T, Delmer D, Somerville C (2001) Modifications of cellulose synthase confer resistance to isoxaben and thiazolidinone herbicides in Arabidopsis Ixr1 mutants. Proc Natl Acad Sci USA **98:** 10079–10084

Schnabelrauch LS, Kieliszewski M, Upham BL, Alizedeh H, Lamport DT (1996) Isolation of pl 4.6 extensin peroxidase from tomato cell suspension cultures and identification of Val-Tyr-Lys as putative intermolecular cross-link site. Plant J **9:** 477–489

Selig MJ, Adney WS, Himmel ME, Decker SR (2009) The impact of cell wall acetylation on corn stover hydrolysis by cellulolytic and xylanolytic enzymes. Cellulose (Lond) **16:** 711–722

Shigeto J, Itoh Y, Hirao S, Ohira K, Fujita K, Tsutsumi Y (2015) Simultaneously disrupting AtPrx2, AtPrx25 and AtPrx71 alters lignin content and structure in Arabidopsis stem. J Integr Plant Biol **57:** 349–356

Shigeto J, Kiyonaga Y, Fujita K, Kondo R, Tsutsumi Y (2013) Putative cationic cell-wall-bound peroxidase homologues in Arabidopsis, AtPrx2, AtPrx25, and AtPrx71, are involved in lignification. J Agric Food Chem **61:** 3781–3788

Shigeto J, Nagano M, Fujita K, Tsutsumi Y (2014) Catalytic profile of Arabidopsis peroxidases, AtPrx-2, 25 and 71, contributing to stem lignification. PLoS One **9:** e105332

Smyth GK (2004) Linear models and empirical Bayes methods for assessing differential expression in microarray experiments. Stat Appl Genet Molec Biol **3:** 1–25

Tan L, Eberhard S, Pattathil S, Warder C, Glushka J, Yuan C, Hao Z, Zhu X, Avci U, Miller JS, et al (2013) An *Arabidopsis* cell wall proteoglycan consists of pectin and arabinoxylan covalently linked to an arabinogalactan protein. Plant Cell **25:** 270–287

Tognolli M, Penel C, Greppin H, Simon P (2002) Analysis and expression of the class III peroxidase large gene family in *Arabidopsis thaliana*. Gene **288:** 129–138

Torres MA, Dangl JL (2005) Functions of the respiratory burst oxidase in biotic interactions, abiotic stress and development. Curr Opin Plant Biol **8:** 397–403

Torres MA, Dangl JL, Jones JD (2002) Arabidopsis gp91phox homologues AtrbohD and AtrbohF are required for accumulation of reactive oxygen intermediates in the plant defense response. Proc Natl Acad Sci USA **99:** 517–522

Tsang DL, Edmond C, Harrington JL, Nühse TS (2011) Cell wall integrity controls root elongation via a general 1-aminocyclopropane-1-carboxylic acid-dependent, ethylene-independent pathway. Plant Physiol **156:** 596–604

Vossen RH, Aten E, Roos A, den Dunnen JT (2009) High-resolution melting analysis (HRMA): more than just sequence variant screening. Hum Mutat **30:** 860–866

Welinder KG, Justesen AF, Kjaersgård IVH, Jensen RB, Rasmussen SK, Jespersen HM, Duroux L (2002) Structural diversity and transcription of class III peroxidases from *Arabidopsis thaliana*. Eur J Biochem **269:** 6063–6081

Willats WG, McCartney L, Mackie W, Knox JP (2001) Pectin: cell biology and prospects for functional analysis. Plant Mol Biol **47:** 9–27

Wolf S, Rausch T, Greiner S (2009) The N-terminal pro region mediates retention of unprocessed type-I PME in the Golgi apparatus. Plant J **58:** 361–375

Zhang GF, Staehelin LA (1992) Functional compartmentation of the Golgi apparatus of plant cells : immunocytochemical analysis of high-pressure frozen- and freeze-substituted sycamore maple suspension culture cells. Plant Physiol **99:** 1070–1083

Zhou N, Tootle TL, Glazebrook J (1999) *Arabidopsis PAD3*, a gene required for camalexin biosynthesis, encodes a putative cytochrome P450 monooxygenase. Plant Cell **11:** 2419–2428

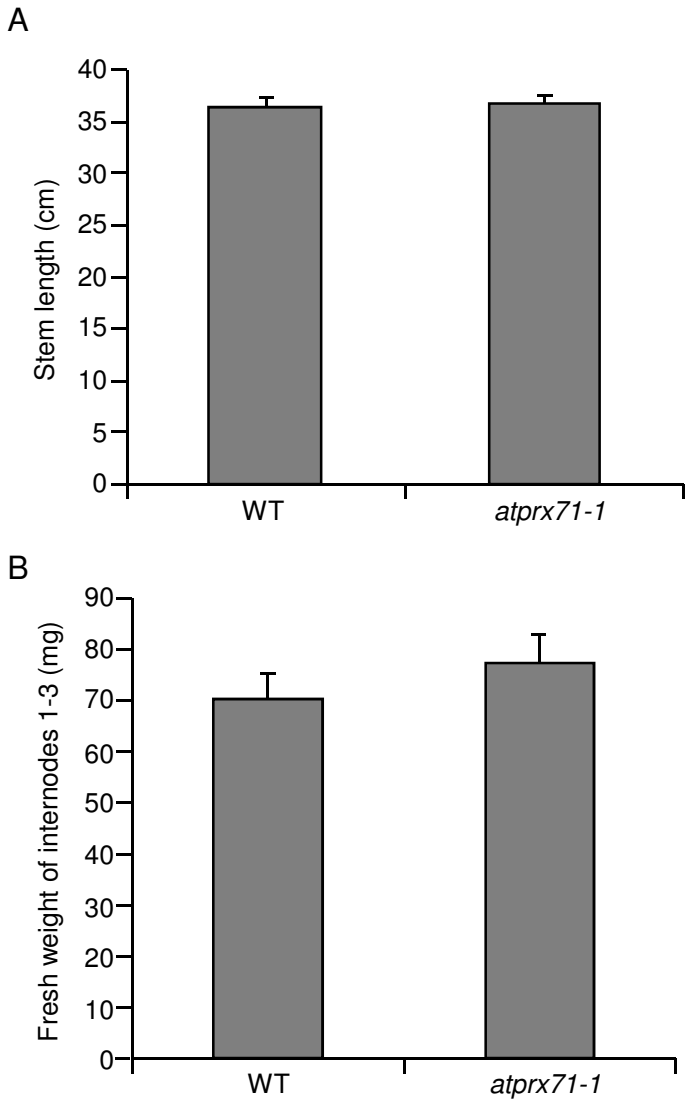

Supplemental Figure S1. Lack of *AtPRX71* does not affect stem growth. Length of the main floral stem (A) and fresh weight of its first, second and third internode (starting from the rosette) of seven-week-old WT and *atprx71-1* soil-grown plants. Bars represent average ± SE (n>15). No significant differences between WT and mutants were observed. This experiment was repeated twice with similar results.

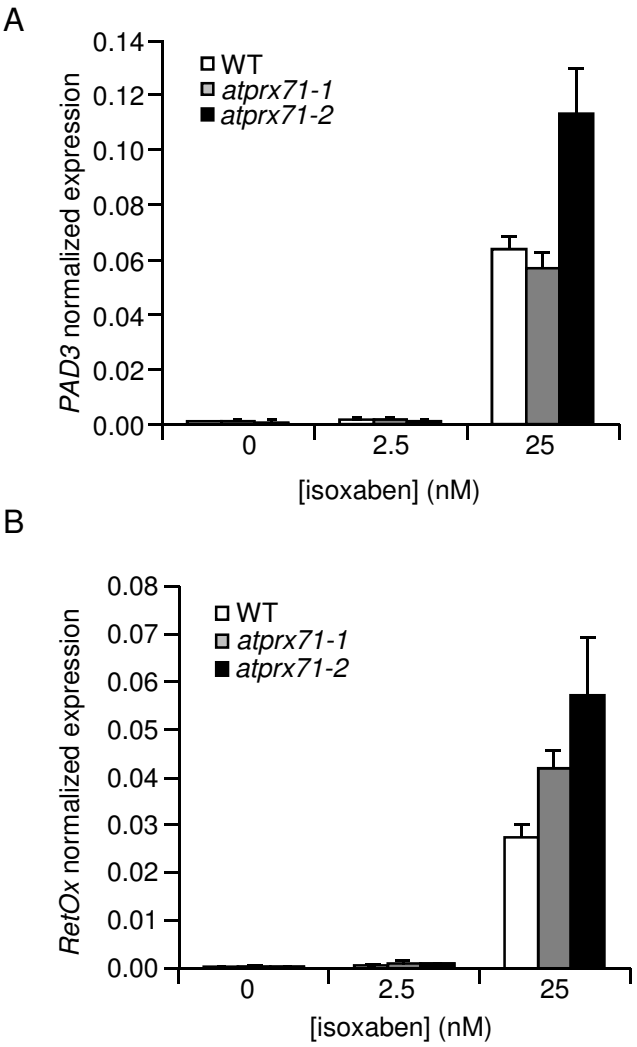

Supplemental Figure S2. Gene expression induced by isoxaben is not altered in *atprx71* plants. Expression of *PAD3* (A) and *RetOx* (B) was analyzed by qPCR using total RNA extracted from WT, *atprx71-1* and *atprx71-2* seedlings grown in liquid medium for 10 days and then treated for 24 h with the indicated doses of isoxaben. Expression was normalized using the *UBQ5* gene. Bars represent average expression ±SD of three technical replicates.

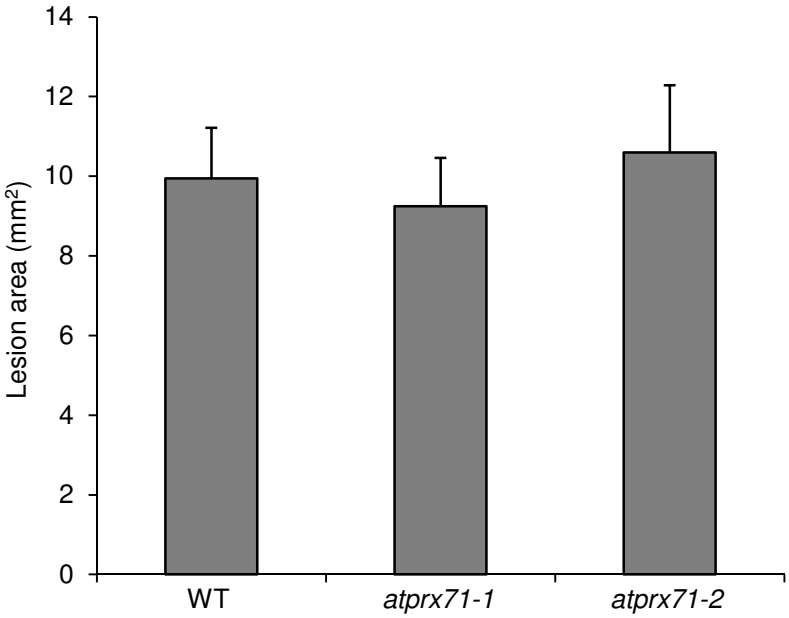

Supplemental Figure S3. *AtPRX71* is not required for basal resistance to *Botrytis cinerea*. Leaves of four-week-old WT and *atprx71-1* (A) or *atprx71-2* (B) plants were inoculated with a *B. cinerea* spore suspension and lesion area was measured after two days. Bars indicate average area ± SE (n>10). Differences between WT and mutants were not significant, according to Student's t-test (P>0.05).

Supplemental Table 1. Differentially expressed proteins in the leaf proteome of *AtECS*1 in comparison to Col-0 as identified by MALDI TOF-TOF MSMS.

SSP no.	Accession no.	Protein [organism]	Fold change	Score	Peptide count	SC (%)	Theoretical Mw (kD) /pI
Carbon metabolism							
1	gi|15220615	CAB1 (CHLOROPHYLL A/B BINDING PROTEIN 1); chlorophyll binding [*A. thaliana*]	0.03	326	10	69	28.28/5.47
2	gi|21593220	33 kDa polypeptide of oxygen-evolving complex (OEC) in photosystem II [*A. thaliana*]	0.29	153	15	53	35.36/5.55
3	gi|16374	chlorophyll a/b binding protein (LHCP AB 180) [*A. thaliana*]	0.04	184	9	71	25.00/5.12
4	gi|15222166	PSBP-1 (OXYGEN-EVOLVING ENHANCER PROTEIN 2); poly(U) binding [*A. thaliana*]	0.05	255	9	43	28.25/6.9
5	gi|21593520	chlorophyll a/b-binding protein-like [*A. thaliana*]	0.47	127	7	32	25.03/5.12
6	gi|7525041	ribulose-1,5-bisphosphate carboxylase/ oxygenase large subunit [*A. thaliana*]	0.05	623	22	55	53.43/5.88
7	gi|18405145	RCA (RUBISCO ACTIVASE) [*A. thaliana*]	0.14	378	20	58	52.35/5.87
8	gi|7525041	ribulose-1,5-bisphosphate carboxylase/ oxygenase large subunit [*A. thaliana*]	26.62	638	23	56	53.4/5.88
9	gi|13926229	F1O19.10/F1O19.10 [*A. thaliana*]	13.97	462	10	72	14.91/5.69
10	gi|30687995	RCA (RUBISCO ACTIVASE) [*A. thaliana*]	2.15	650	18	54	49.35/7.55
11	gi|18405145	RCA (RUBISCO ACTIVASE) [*A. thaliana*]	3.02	222	15	47	52.34/5.87
12	gi|15219826	RBCS1A; ribulose-bisphosphate carboxylase [*A. thaliana*]	3.04	225	11	67	20.48/7.59
13	gi|15219826	RBCS1A; ribulose-bisphosphate carboxylase [*A. thaliana*]	2.69	316	12	64	20.48/7.59
14	gi|13926229	F1O19.10/F1O19.10 [*A. thaliana*]	2.49	636	13	90	14.91/5.69
15	gi|140325934	ATPase alpha subunit [*Brassica juncea*]	0.46	243	14	32	55.33/6.01
16	gi|17939849	mitochondrial F1 ATP synthase beta subunit [*A. thaliana*]	5.45	612	26	65	63.55/6.52
17	gi|7525040	ATP synthase CF1 beta	2.45	794	25	67	53.95/5.38

		subunit [*A. thaliana*]					
18	gi|7525018	ATP synthase CF1 alpha subunit [*A. thaliana*]	2.41	373	20	45	55.35/5.19
19	gi|1022805	phosphoglycerate kinase [*A. thaliana*]	64.88	240	11	45	41.99/4.93
20	gi|15240578	cpHSC70-2 (HEAT SHOCK PROTEIN 70-7); ATP binding / unfolded protein binding [*A. thaliana*]	22.65	252	13	22	77.06/5.17
21	gi|15219234	VHA-A; ATP binding / hydrogen ion transporting ATP synthase, rotational mechanism [*A. thaliana*]	1.56	125	16	33	69.11/5.11
Stress and defense							
22	gi|15220604	ABC transporter I family member 17 [*A. thaliana*]	0.03	66	9	53	29.9/6.04
23	gi|15241492	FDH (FORMATE DEHYDROGENASE); NAD binding /binding / catalytic/ cofactor binding / oxidoreductase, [*A. thaliana*]	0.01	462	18	55	42.67/7.12
24	gi|15231702	ATMDAR1 (MONODEHYDROASCORBATE REDUCTASE 1); monodehydroascorbatereductase (NADH) [*A. thaliana*]	0.25	93	11	37	46.6/6.41
25	gi|15226973	GDCH (Glycine decarboxylase complex H) [*A. thaliana*]	0.08	96	7	61	18.04/5.24
26	gi|28973653	putative TPR-repeat protein [*A. thaliana*]	0.48	62	10	23	64.76/5.85
27	gi|238027922	Peptidyl-prolylcis-trans isomerase A [*Burkholderiaglumae* BGR1]	2.96	49	5	29	20.49/9.25
28	gi|15241844	BIP1; ATP binding [*A. thaliana*]	2.07	193	15	26	73.83/5.08
29	gi|397482	heat shock protein 70 cognate [*A. thaliana*]	23.62	480	24	49	71.72/5.03
30	gi|397482	heat shock protein 70 cognate [*A. thaliana*]	34.82	523	27	52	71.72/5.03
31	gi|15229033	MTO3 (S-adenosylmethionine synthase 3); methionine adenosyltransferase[*A. thaliana*]	21.95	337	17	55	43.16/5.51
32	gi|15223576	DHAR1 (DEHYDROASCORBATE REDUCTASE); glutathione dehydrogenase (ascorbate) [*A. thaliana*]	2.12	255	10	70	23.74/5.56
33	gi|21555831	peptidylprolylisomeraseROC4 [*A. thaliana*]	15.18	92	8	44	28.52/8.83

34	gi|15240578	cpHSC70-2 (HEAT SHOCK PROTEIN 70-7); ATP binding / unfolded protein binding [*A. thaliana*]	22.65	252	13	22	77.06/5.17
35	gi|975646	dehydrin[*A. thaliana*]	2.18	95	11	67	29.91/4.78
36	gi|42573371	CA2 (BETA CARBONIC ANHYDRASE 2); carbonate dehydratase/ zinc ion binding [*A. thaliana*]	3.64	214	5	29	28.66/5.36
37	gi|21555831	peptidylprolylisomerase ROC4 [*A. thaliana*]	2.2	383	9	44	28.52/8.83
38	gi|3341717	ACC oxidase [*A. thaliana*]	3.12	47	12	45	36.16/4.97
39	gi|15231718	peroxiredoxin type 2, putative [*A. thaliana*]	2.11	115	8	44	24.78/9.12
40	gi|21553667	2-cys peroxiredoxin-like protein [*A. thaliana*]	1576	84	5	25	29.66/5.71
41	gi|625155	cold stress protein [*A. thaliana*]	487.6	46	5	50	11.42/7.26
42	gi|58177602	Chain A, X-Ray Structure Of Annexin Gene At1g35720 [*A. thaliana*]	1.45	380	14	59	36.25/5.21
Others							
43	gi|15227376	ATSFGH (ARABIDOPSIS THALIANA S-FORMYLGLUTATHIONE HYDROLASE); S-formylglutathione hydrolase [*A. thaliana*]	0.27	187	13	68	31.92/5.91
44	gi|30696056	LOS1 (Low expression of osmotically responsive genes 1) [*A. thaliana*]	0.26	58	13	19	94.7/5.89
45	gi|47600741	cobalamin-independent methionine synthase [*A. thaliana*]	2.13	362	21	37	84.60/6.09

Supplemental Table 2. Differentially expressed proteins in the leaf proteome of *pad2-1* in comparison to Col-0 as identified by MALDI TOF-TOF MSMS.

SSP no.	Accession no.	Protein [organism]	Fold change	Score	Peptide count	SC (%)	Theoretical Mw (kD) /pI
Carbon metabolism							
46	gi|7525041	ribulose-1,5-bisphosphate carboxylase/ oxygenase large subunit [*A. thaliana*]	0.22	219	17	44	53.4/5.88
47	gi|336390	glyceraldehyde 3-phosphate dehydrogenase B subunit [*A. thaliana*]	0.2	305	15	38	43.16/5.6
48	gi|222424528	AT3G54890 [*A. thaliana*]	0.44	136	5	28	17.65/6.1

49	gi|15228983	thylakoid lumenal 20 kDa protein [*A. thaliana*]	0.89	65	9	45	28.72/9.3
Energy metabolism							
50	gi|15237054	TUF (VACUOLAR ATP SYNTHASE SUBUNIT E1) [*A. thaliana*]	0.46	171	15	54	26.27/6.04
51	gi|7525040	ATP synthase CF1 beta subunit [*A. thaliana*]	2.03	856	24	64	53.95/5.38
52	gi|15219234	VHA-A; ATP binding / hydrogen ion transporting ATP synthase, rotational mechanism [*A. thaliana*]	44.85	411	27	52	69.11/5.11
Stress and defense							
53	gi|20197312	glutathione S-transferase (GST6) [*A. thaliana*]	0.12	64	5	34	24.12/6.09
54	gi|79325249	FSD1 (FE SUPEROXIDE DISMUTASE 1); iron superoxide dismutase [*A. thaliana*]	0.49	102	5	32	21.08/6.16
55	gi|62320917	carbonic anhydrase, chloroplast precursor [*A. thaliana*]	0.42	588	14	62	28.5/5.29
56	gi|227204455	AT2G37660 [*A. thaliana*]	0.43	333	8	39	26.3/5.29
57	gi|30685030	CA2 (BETA CARBONIC ANHYDRASE 2); carbonate dehydratase/ zinc ion binding [*A. thaliana*]	0.44	65	16	28	28.66/5.36
58	gi|42573371	CA2 (BETA CARBONIC ANHYDRASE 2); carbonate dehydratase/ zinc ion binding [*A. thaliana*]	0.04	175	9	57	28.66/5.36
59	gi|15231718	peroxiredoxin type 2, putative [*A. thaliana*]	0.07	74	6	37	24.78/9.12
60	gi|4586021	cytoplasmic aconitatehydratase[*A. thaliana*]	0.11	204	23	38	98.7/5.79
61	gi|79328685	TGG2 (GLUCOSIDE GLUCOHYDROLASE 2); hydrolase, hydrolyzing O-glycosyl compounds [*A. thaliana*]	0.47	203	15	35	53.9/6.43
62	gi|166574	60-kDa chaperonin-60 alpha-polypeptide [*A. thaliana*]	0.08	116	8	45	25.98/4.89
63	gi|23397152	putative heat shock protein 81-2 (HSP81-2) [*A. thaliana*]	0.14	413	30	45	80.32/4.95
64	gi|15218382	PATL1 (PATELLIN 1); transporter [*A. thaliana*]	0.04	264	20	36	64.12/4.82
65	gi|15241844	BIP1; ATP binding [*A. thaliana*]	0.14	345	21	35	73.86/5.08
66	gi|3341717	ACC oxidase [*A. thaliana*]	0.42	69	10	39	36.16/4.97
Others							

67	gi|225431585	PREDICTED: hypothetical protein [*Vitisvinifera*]	0.06	246	12	47	41.9/5.31
68	gi|21536745	ferritin 1 precursor [*A. thaliana*]	0.4	362	11	41	28.15/5.73
69	gi|487791	GF14omega isoform [*A. thaliana*]	0.03	125	9	40	29.2/4.71
70	gi|225443399	PREDICTED: hypothetical protein [*V. vinifera*]	2.16	155	17	36	68.96/5.24
71	gi|226499128	long-chain-fatty-acid-CoA ligase-like protein [*Zea mays*]	2.03	75	13	26	61.54/6.23

Supplemental Table 3. List of primers used.

Gene	**Forward primer (5'- 3')**	**Reverse primer (5'- 3')**
γ-ECS	AATCTAGATATGGCCTTGATGTCCAGGC	AAGAGCTCAATCAGTAGAGAAGCTCCTCAAA
γ-ECS-700bp	AATATTTCTTCACGGAATTCCTC	AAGAGAGCTGTAGCAATAGGC
*npt*II	GAGGCTATTCGGCTATGACTG	ATCGGGAGGGGCGATACCGTA
*PR*1	ATGAATTTTACTGGCTATTCTCGATT	ATGTACGTGTGTATGCATGATCAC
*ACS*1	ATGTCTCAGGGTGCATGTGA	CCGCCGTACAAATAGATGCC
*ACS*2	GGGTCTTCCGGGAAAAAATAAAG	TTGGAAATTAGCGATGTCGCTAAA
*ACS*4	ACGACGTTACCAAGAACCCT	GAAGGAAGAGAGGCCATGGT
*ACS*5	CCGGGTTGGTTTAGGGTTTG	CACGATCGGTCCATGAAACC
*ACS*6	ATGGTGGCTTTTGCAACAGAGAA	CAATGTCACTGAATTGATTCACAC
*ACS*7	TGTTTGAAAGGGAACGCAGG	TTCGTCGGTCCATGAACTCA
*ACS*8	TTTTCGCGTTGGGGTGATTT	TGTCTGTTCTTGAGCCGGAT
*ACS*9	AAATGGAGAACGGGAGCAGA	AAGAGGGTTAGACGGGTTGG
*ACS*10	CGTTCCATGTAGAAGTGCGG	TCACGGGCAAAGTCCAAAAG
*ACS*11	CCAGGCTCATCGTGTCATTG	AGAGGAAAGCTTGGAGACCC
*ACO*1	GATCAAAGAGAGAGAGATGGAGA	TGAAATGTTTGGGATCTGACAGAT
*ACO*2	ATGGAGAAGAACATGAAGTTTCCA	AGAAAGTGCTTTCCCAATCGAC
*proACS*2	ATTAAGCTTCAAACAAAAAGTTC	ATTCCATGGTGCTGTGTCAATTCTCAC

	TTCTTAGAC	TTC
*proACS*6	ATAGGATCCCTAAAAATGTAGAG ACAGATGGA	ATTCCATGGCTTCTTTAATATAGGTTT CTTTTG
*proACO*1	TTAGGCCTCTTTTGGCTTGTTTAG TTTGGAG	TTACCGGTTTATTTACTTTTTCTCACA CACAG
*MPK*3	ATGAACACCGGCGGTGGCCA	ATGATCAAGATGACGAAGAAGCTT
*MPK*6	CGGTGGTTCAGGTCAACCGG	AATTTTCTTAATCGCAACGCTCTC
*MKK*4	TGAAAAGCCGTCCCCGTCGC	TATACCGTTCCACCTGCTCCG
*MKK*5	AAACCGATTCAATCTCCTTCTGG	CGTGACGTCGGAGTGTGGATT
*MKK*9	GGCTTTAGTACGTGAACGTCGT	CCATCTCTCGCATCAACTGTC
GUS	GTAGAAACCCCAACCCGTGA	AGTCTGCCAGTTCAGTTCGTT
actin	GGCTGATGGTGAAGATATTCAAC	CATTGTAGAAAGTATGATGCCAGA
WRKY33	ATTGAATTCATGGACAATAGCAG AACCAGACAA	ATTCCATGGTCAGGGCATAAACGAAT CGAAAAA
*pACS*2 (ChIP)	AGGCCATAAGCCCATTCAAA	GCCTACAGTGCACGACTTCA
*pACS*6 (ChIP)	AAAGTCGTTGAGATTGTGTTGG	TGGCAGCCTTAAAGACCAGT